```
10 REM R=ARGON  O=CO  S=CH4  T=CO2  MCMA=MOLES CO/MOLE AR FED
20 REM  X=RXN TEMP,KELVINS  RA=H2/CO RATIO FED(EFFECTIVE RATIO FOR CYCLE)
25 REM PMCMA=MCMA DURING PRECARBID.   SMCMA=MCMA DURING SYNTHESIS
30 REM PRA=RA DURING PRECARB.         SRA=RA DURING SYNTHESIS
35 DIM R(50),O(50),S(50),T(50),A(50),B(50),C(50),D(50),E(50)
40 DIM F(50),G(50),H(50),Q(50),U(50),V(50),W(50),L(50)
50 DIM X(50),Y(50),Z(50)
60 REM*****PLACE THE DATE & COMMENTS ON THE NEXT 2 LINES*********
70 L$="9/25/84"
80 LM$="STEADY STATE EXPERIMENT F-5    "
83 LR$=" THIS EXPERIMENT USES 1.03:1 S-GAS FOR A 22 MINUTE RUN "
85 LS$=" AFTER FIRST EXPOSING IT TO 4:1 PRECARB. GAS FOR 2 HOURS.      "
87 LT$="
90 REM +++++++SPECIFY INPUT AND OUTPUT FILE NAMES AND PARAMETERS+++++++++
100 LP$="EXF5.DAT"
110 LO$="RESF5.DAT"
115 NN=3
120 N=3
125 REM                              INPUT PARAMETERS!
128 PMCMA=10.682
129 SMCMA=10.382
130 REM SMCMA=7.745
135 PRA=4.0
140 SRA=1.03
150 K=648
151 REM ***************************************************************
152 MCMA=PMCMA
154 RA=PRA
160 REM ***READ IN INTEGRATED PEAK AREAS**********************************
170 OPEN "I",1,LP$
180 FOR I=1 TO N
190 INPUT#1,R(I),O(I),S(I),T(I)
200 NEXT I
210 CLOSE#1
220 REM ***WEIGHT THE PEAK AREAS USING TC WEIGHT FACTORS*********
230 FOR I=1 TO N
235 IF I>NN THEN MCMA=SMCMA
240 R(I)=R(I)*.95
250 O(I)=O(I)*.67
260 S(I)=S(I)*.45
270 T(I)=T(I)*.915
280 REM ***MOLES CO CONVERTED/MOLE AR*****************************
290 A(I)=MCMA-(O(I)/R(I)*1.436)
300 REM ***MOLES CH4/MOLE AR*************************************
310 B(I)=(S(I)/R(I)*2.49)
320 REM ***MOLES CO2/MOLE AR*************************************
330 C(I)=(T(I)/R(I)*.9077)
340 REM ***MOLES CH4 PRODUCED/MOLE CO CONVERTED*******************
350 D(I)=B(I)/A(I)
360 REM ***MOLES CO2 PRODUCED/MOLE CO CONVERTED******************
370 E(I)=C(I)/A(I)
380 NEXT I
390 FOR I=1 TO N
395 MCMA=PMCMA
395 IF I>NN THEN MCMA=SMCMA
400 REM ***CO CONVERSION, CO UNCONVERTED*************************
410 F(I)=A(I)/MCMA
420 G(I)=1!-F(I)
430 REM ***CO2 PRODUCED, CH4 PRODUCED****************************
440 H(I)=F(I)*E(I)
450 Q(I)=F(I)*D(I)
460 REM ***IMPLIED MOLES OF -CH2-  ******************************
470 U(I)=1!-(G(I)+H(I)+Q(I))
480 REM ***IMPLIED MOLES OF H2O  ********************************
490 V(I)=1!-(2*H(I)+G(I))
500 REM ***IMPLIED MOLES OF H2 USED*****************************
510 W(I)=(2*U(I)+4*H(I)+2*V(I))/2!
520 REM *** H2/CO USAGE RATIO ***********************************
530 X(I)=W(I)/F(I)
540 REM *** CALCULATED EQUILIBRIUM CONSTANT FOR WATER-GAS SHIFT*****
550 Y(I)=.0102*EXP(4730/K)
560 REM *** EXPERIMENTAL EQUILIBRIUM CONSTANT FOR WATER-GAS SHIFT****
562 RA=PRA
```

Figure C.2 A Microcomputer Program (MASSBAL.BAS) Used to Compile the Data Obtained From the Light-Gas Analysis.

```
565 IF I>NN THEN RA=SRA
570 Z(I)=(H(I)*(RA-W(I))/(G(I)*V(I)))
580 REM ***IMPLIED CONVERSION OF HYDROGEN**********************************
590 L(I)=W(I)/RA
600 NEXT I
610 OPEN "O",2,L$
620 PRINT#2,"DATE OF EXPERIMENT ",L$,LM$
630 PRINT "DATE OF EXPERIMENT ",L$,LM$
631 PRINT#2," "
632 PRINT#2,LR$
633 PRINT#2,LS$
634 PRINT#2,LT$
640 PRINT#2," "
650 PRINT
660 PRINT#2,"TEMPERATURE=",K,"# DATA PTS.=",N
670 PRINT   "TEMPERATURE=",K,"# DATA PTS.=",N
680 PRINT#2," "
690 PRINT
700 PRINT#2," SAMPLE "," CO CONV","CO2/CO","CH4/CO"," CO/AR"," H2/CO"
710 PRINT   " SAMPLE "," CO CONV","CO2/CO","CH4/CO"," CO/AR"," H2/CO"
720 PRINT#2," NUMBER "," ","CONV "," CONV "," FED "," RATIO"
730 PRINT   " NUMBER "," ","CONV "," CONV "," FED "," RATIO"
740 FOR I=1 TO N
742 RA=PRA
743 IF I>NN THEN RA=SRA
744 MCMA=PMCMA
745 IF I>NN THEN MCMA=SMCMA
750 PRINT#2,I,F(I),E(I),D(I),MCMA,RA
760 PRINT   I,F(I),E(I),D(I),MCMA,RA
770 NEXT I
780 PRINT#2," "
790 PRINT
800 PRINT#2," "
810 PRINT
820 PRINT#2," SAMPLE ","H2 CONV"," -CH2-","  H2O"," H2 USED","H2/CO"
830 PRINT   " SAMPLE ","H2 CONV"," -CH2-","  H2O"," H2 USED","H2/CO"
840 PRINT#2," NUMBER","IMPLIED","IMPLIED","IMPLIED","IMPLIED","USAGE"
850 PRINT   " NUMBER","IMPLIED","IMPLIED","IMPLIED","IMPLIED","USAGE"
860 FOR I=1 TO N
870 PRINT#2,I,L(I),U(I),V(I),W(I),X(I)
880 PRINT   I,L(I),U(I),V(I),W(I),X(I)
890 NEXT I
900 PRINT#2," "
910 PRINT
920 PRINT#2," "
930 PRINT
940 PRINT#2," SAMPLE "," -CH2- ","CALC KEQ","EXPT KEQ","SUM=1?"
950 PRINT   " SAMPLE "," -CH2- ","CALC KEQ","EXPT KEQ","SUM=1?"
960 PRINT#2," NUMBER "," /CO CONV  "
970 PRINT   " NUMBER "," /CO CONV  "
980 FOR I=1 TO N
985 UPRIME=U(I)/F(I)
994 SUM=UPRIME+E(I)+D(I)
999 PRINT#2,I,UPRIME,Y(I),Z(I),SUM
1000 PRINT   I,UPRIME,Y(I),Z(I),SUM
1010 NEXT I
1020 CLOSE#2
```

Figure C.2 (Continued)

```
10 REM  THIS PROGRAM CALCULATES THE NUMBER OF MOLES OF A SPECIFIC HYDRO-
20 REM   CARBON (OR FUSED PEAK OF HC'S) FROM THE INTEGRATED PEAK AREAS
30 REM   ON THE CHROMATOGRAM.  ASSUMPTIONS= 1) FUSED C2 AND C3 PEAKS
40 REM   USE THE AVERAGE MOL. WT. TO CALCULATE MOLES CONVERTED.
50 DIM A(24),B(24),C(24),D(24),E(24),F(24),G(24),H(24),J(24),K(24),M(24)
51 DIM Q(24),R(24)
60 REM   X=MOLES CH4 PRODUCED PER MOLE CO CONVERTED  XX=FLOW RATE IN SCCM
65 REM   YY=FRACTION CO IN S-GAS FEED  ZZ=CO CONVERTED/CO FED
66 REM   WW=RATIO OF S-GAS FEED DURATION TO TOTAL FEED DURATION(S+F)
67 REM      [VALUE OF WW FOR STEADY-STATE REACTION IS 1.0]
68 REM   HH=MOLES OF CO2 PRODUCED/ MOLE CO CONV.
70 L$="8/10/84"
80 LM$="STEADY STATE W/O PRECARB."
90 LM$="HPRESB3.DAT"
100 LP$="HPB3.DAT"
101 LT$="EXPERIMENT B-3: THIS EXPERIMENT CONSISTS OF 10 HOURS "
103 LS$="OF 4.0:1 S-GAS FLOW AT 633K.                        "
110 X=.1791
102 XX=220
104 YY=0.1925
106 ZZ=.9268
107 WW=1.0
108 HH=0.2073
109 GOSUB 1400
120 REM INPUT INTEGRATED PEAK AREAS FOR OLEFINS AND PARAFINS
130 OPEN "I",1,LP$
140 FOR I=1 TO 24
150 INPUT#1,A(I)
160 NEXT I
170 CLOSE#1
180 REM  NORMALIZED PEAK AREAS
190 FOR I=1 TO 24
200 D(I)=A(I)/A(I)
210 Z=Z+D(I)
220 NEXT I
230 REM  CALCULATE THE WEIGHT FRACTION OF EACH SPECIES
240 FOR I=1 TO 24
250 B(I)=D(I)/Z
260 NEXT I
270 GOSUB 590
280 REM  CALCULATE MOLES HYDROCARBON PRODUCED PER MOLE CO CONSUMED, C(I)
290 FOR I=1 TO 24
300 C(I)=D(I)*M(I)*X/M(I)
310 IF I=1 THEN E(I)=C(I) ELSE
320 IF I=2 THEN E(I)=C(I)*2 ELSE
330 IF I=3 THEN E(I)=C(I)*3 ELSE
340 IF I<3 THEN IF I<5 THEN E(I)=C(I)*4  ELSE
350 IF I<7 THEN IF I<12 THEN E(I)=C(I)*5  ELSE
360 IF I<11 THEN IF I<15 THEN E(I)=C(I)*6  ELSE
370 IF I<14 THEN IF I<19 THEN E(I)=C(I)*7  ELSE
380 IF I<18 THEN IF I<21 THEN E(I)=C(I)*8  ELSE
390 IF I<20 THEN IF I<23 THEN E(I)=C(I)*9  ELSE
400 IF I<22 THEN E(I)=C(I)*10 ELSE
410 T=T+E(I)
420 NEXT I
421 GOSUB 1500
422 GOSUB 900
430 OPEN "O",2,LQ$
440 PRINT#2,"DATE OF EXPERIMENT",L$,LM$
450 PRINT   "DATE OF EXPERIMENT",L$,LM$
451 PRINT#2," "
452 PRINT#2,LT$
455 PRINT#2,LS$
460 PRINT#2," "
470 PRINT " "
480 PRINT#2,"PEAK #","NORM AREA","WT FRACT.","HC/CO CONV","RATE PROD","M.W."
490 PRINT  "PEAK #","NORM AREA","WT FRACT.","HC/CO CONV","RATE PROD","M.W."
500 FOR I=1 TO 24
510 PRINT#2,I,D(I),B(I),C(I),Q(I),M(I)
520 PRINT I,D(I),B(I),C(I),Q(I),M(I)
530 NEXT I
531 PRINT#2," "
532 PRINT " "
```

Figure C.3 A Microcomputer Program (HEAVY.BAS) Used to Compile the Data Obtained From the Capillary Column Analysis.

```
530 PRINT#2,"CARBON #","MOLES C#","MOLFRC C#","WT C#","WTFRAC C#","RATE C#"
534 PRINT "CARBON #","MOLES C#","MOLFRC C#","WT C#","WTFRAC C#","RATE C#"
535 FOR I=1 TO 10
536 PRINT#2,I,F(I),G(I),H(I),J(I),R(I)
537 PRINT I,F(I),G(I),H(I),J(I),R(I)
538 NEXT I
540 W=Z+A(1)
541 PRINT#2,"  "
542 PRINT "  "
543 PRINT#2,"  "
544 PRINT "  "
550 PRINT#2,"TOTAL PEAK AREA=",W
560 PRINT  "TOTAL PEAK AREA=",W
562 PRINT#2,"TOTAL MOLE CARBON PRODUCED AS OLE&PAR/MOLE CO CONV=",T
563 PRINT  "TOTAL MOLE CARBON PRODUCED AS OLE&PAR/MOLE CO CONV=",T
564 PRINT#2,"MOLE RATIO C1/(C2-C6)=",S1
565 PRINT  "MOLE RATIO C1/(C2-C6)=",S1
566 PRINT#2,"WEIGHT FRACTION C1/(C2-C5)",S2
567 PRINT  "WEIGHT FRACTION C1/(C2-C5)",S2
568 PRINT#2,"RATES ARE IN UNITS OF MMOLES PER HOUR"
569 PRINT#2,"AVG MOL WTS ARE USED FOR C2 AND C3 HYDROCONS DUE TO FUSED PEAKS"
570 GO=T+HH
571 PRINT#2,"TOT MOLE C PRODUCED AS CO2 AND OLE&PARA/MOLE CO CONV=",GO
575 CLOSE#2
580 STOP
590 REM ASSIGN MOLECULAR WEIGHTS TO THE PEAKS
600 C=12.011
610 H=1.008
620 M(1)=C+3*H
630 REM MUST AVG NEXT 2 SETS OF PEAKS. OLEFIN & PARAFIN CUMMINED
640 M(2)=C*2+H*5
650 M(3)=C*3+H*7
660 M(4)=C*3+H*8
670 M(5)=C*4+H*10
680 M(6)=C*4+H*8
690 M(7)=C*3+H*6
700 M(8)=C*3+H*10
710 M(9)=C*5+H*12
720 M(10)=C*5+H*10
730 M(11)=C*5+H*10
740 M(12)=C*6+H*12
750 M(13)=C*6+H*14
760 M(14)=C*6+H*12
770 M(15)=C*7+H*14
780 M(16)=C*7+H*16
790 M(17)=C*7+H*14
800 M(18)=C*7+H*14
810 M(19)=C*8+H*16
820 M(20)=C*8+H*18
830 M(21)=C*9+H*18
840 M(22)=C*9+H*20
850 M(23)=C*10+H*20
860 M(24)=C*10+H*22
870 RETURN
900 REM CALCULATE THE MOLES OF EACH CARBON # FRACTION AND MOLE%
910 F(1)=C(1)
920 F(2)=C(2)
930 F(3)=C(3)
940 F(4)=C(4)+C(5)+C(6)+C(7)
950 F(5)=C(8)+C(9)+C(10)+C(11)
960 F(6)=C(12)+C(13)+C(14)
970 F(7)=C(15)+C(16)+C(17)+C(18)
980 F(8)=C(19)+C(20)
990 F(9)=C(21)+C(22)
1000 F(10)=C(23)+C(24)
1010 FOR I=1 TO 24
1020 MT=MT+C(I)
1030 NEXT I
1040 FOR I=1 TO 10
1050 G(I)=F(I)/MT
1060 NEXT I
1100 WT=0
```

Figure C.3 (Continued)

```
1110 H(1)=B(1)
1120 H(2)=B(2)
1130 H(3)=B(3)
1140 H(4)=B(4)+B(5)+B(6)+B(7)
1150 H(5)=B(8)+B(9)+B(10)+B(11)
1160 H(6)=B(12)+B(13)+B(14)
1170 H(7)=B(15)+B(16)+B(17)+B(18)
1180 H(8)=B(19)+B(20)
1190 H(9)=B(21)+B(22)
1200 H(10)=B(23)+B(24)
1210 FOR I=1 TO 24
1220 WT=WT+B(I)
1230 NEXT
1240 FOR I=1 TO 10
1250 J(I)=H(I)/WT
1260 NEXT I
1270 FOR I=2 TO 14
1280 QT=QT+C(I)
1290 RT=RT+B(I)
1300 NEXT I
1310 S1=C(1)/(QT)
1320 S2=B(1)/(RT)
1330 RETURN
1400 REM THIS SUBROUTINE CALCULATES THE MMOLES OF CO CONVERTED PER HR
1410 REM NN=NUMBER OF MMOLES CO FED/HR  TT=MMOLES OF CO CONVERTED/HR
1412 REM    XX=FLOW RATE IN LCCM
1413 REM    YY=FRACTION CO IN S-GAS FEED  ZZ=CO CONVERTED/CO FED
1415 REM    WW=RATIO OF S-GAS FEED DURATION TO TOTAL FEED DURATION(S+F)
1420 NN=(XX/(92.04*273))*1000*60*YY*WW
1430 TT=NN*ZZ
1440 RETURN
1500 REM    THIS SUBROUTINE CALCULATES THE RATE OF PRODUCTION OF EACH
1510 REM     PRODUCT IN MMOLES PER HOUR .Q(I).  THE RATE OF PRODUCTION
1515 REM     OF EACH SPECIES IN TERMS OF CARBON NUMBER IS ALSO FOUND. R(I).
1518 FOR I=1 TO 24
1520 Q(I)=C(I)*TT
1530 NEXT I
1540 R(1)=Q(1)
1550 R(2)=Q(2)
1560 R(3)=Q(3)
1570 R(4)=Q(4)+Q(5)+Q(6)+Q(7)
1580 R(5)=Q(8)+Q(9)+Q(10)+Q(11)
1590 R(6)=Q(12)+Q(13)+Q(14)
1600 R(7)=Q(15)+Q(16)+Q(17)+Q(18)
1610 R(8)=Q(19)+Q(20)
1620 R(9)=Q(21)+Q(22)
1630 R(10)=Q(23)+Q(24)
1700 RETURN
```

Figure C.3 (Continued)

APPENDIX D

Safety Provisions for the Fischer-Tropsch Synthesis Microreactor System

Location of the Microreactor System

The vibrofluidized microreactor system described in Section 5.1 is located in the Laboratory for Coal Science and Process Chemistry ("coal lab"), Room 319A, on the third floor, northeast wing of Randolph Hall, Virginia Polytechnic Institute and State Unviersity. Above the microreactor system is the building roof, and below it is the Unit Operations Laboratory ("U.O. Lab"). Figure D.1 shows a schematic of the location of the microreactor system ("reactor lab"). The system is surrounded by cinderblock walls on three sides, and by plywood on the fourth side and on the top, forming a "reactor box" as labelled in Figure D.1. The dimensions of this reactor box are 1.45 m × 2.13 m (width × length × height), giving a total volume of 4.0768 m^3. The laboratory surrounding this box, labelled as "reactor lab" in Figure D.1, has the dimensions of 3.5 m × 7 m × 4.5 m or a total voluime of 84.53 m^3.

Ventilation of the Microreactor System

Ventilation for the entire reactor laboratory is provided by a large roof-fan which draws air from both the coal laboratory and the unit operations laboratory. This roof-fan draws air at a volumetric flow rate of approximately 9.46×10^{-3} m^3/sec (0.334 ft^3/sec or 20.04 cfm) at the grate of the reactor laboratory. Thus, the entire air content of the reactor laboratory would be replaced approximately once every two and one-half hours if there was no other air exit. However, an additional vent fan draws air from the reactor box at a faster rate of 9.91×10^{-2} m^3/sec (3.5 ft^3/sec or 2,100 cfm). This means that the air content in the reactor box can be replaced approximately once every 41 seconds. Also, the entire

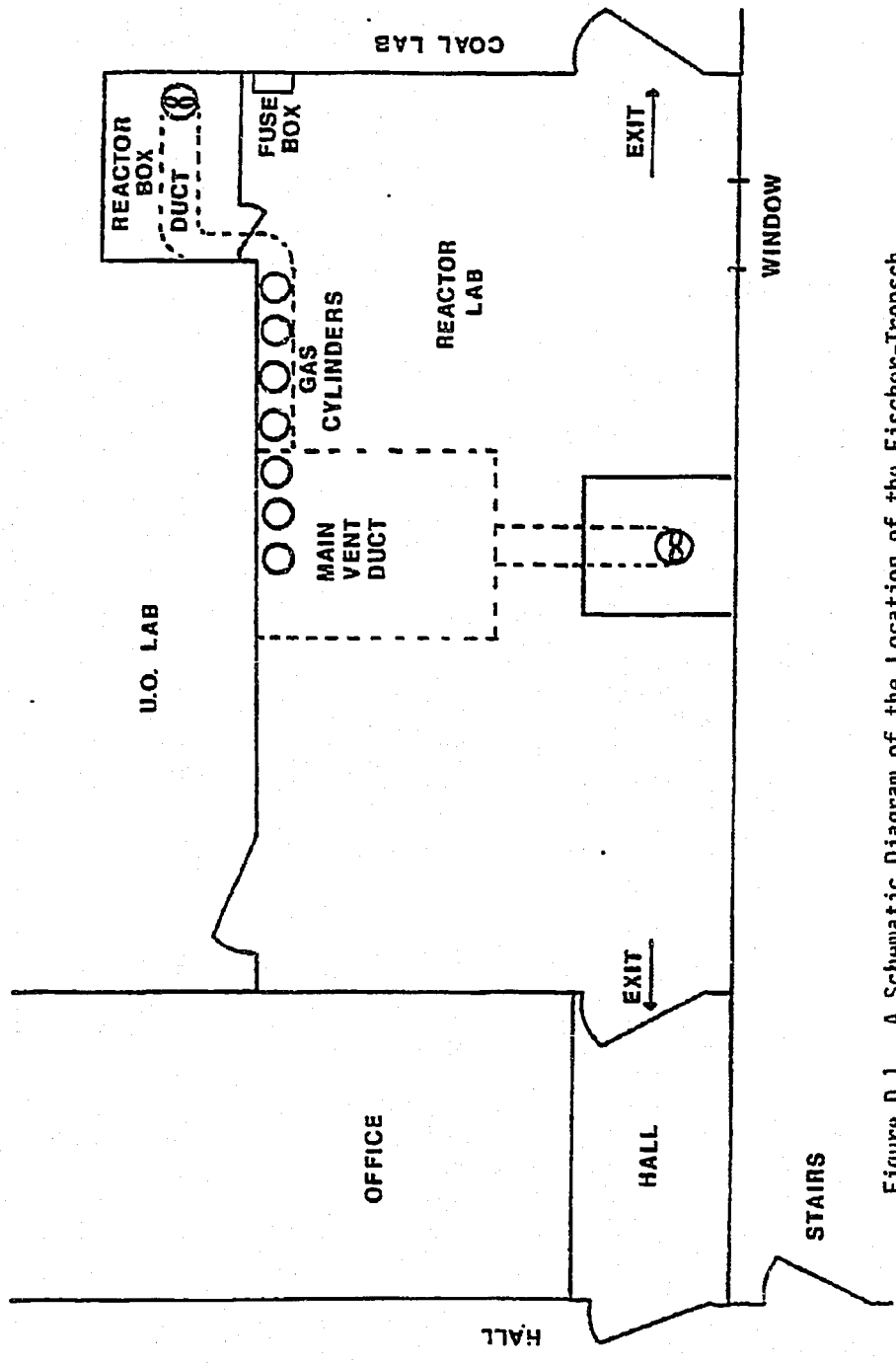

Figure D.1. A Schematic Diagram of the Location of the Fischer-Tropsch Synthesis Microreactor System.

room air in the reactor laboratory is replace about once every 7 minutes. Note that fresh air is drawn into the reactor laboratory via the unit operations laboratory and an air duct in the coal laboratory.

The reactor box has been caulked with silicone rubber at all of its joints and around the edges of the plexiglass at the roof light. The small piece of plywood covering a vent hole in the wall has also been carefully caulked. The roof light is located on top of the reactor box and shines light through the plexiglass to eliminate any possibility of spark hazard.

Table D.1 summarizes the estimated volumes of different components of the microreactor system and the estimated air renewal rates of the reactor box and the reactor laboratory. The American Conference of Governmental Industrial Hygienists has recommended a threshold limit value of 50 ppm for CO representing the concentration of CO in air to which nearly all workers may be continuously exposed without adverse effects.

The flammable limit of H_2 in air is 4 to 75% by volume, depending upon the surrounding situations.

High Temperature and Pressure Precautions

The vibrofluidized microreactor system is to be run at pressures up to 3030 kPa and parts of the system at temperatures up to 450°C. Thus, the upper limits of operating temperatures and pressures of different system components must be known. Those are summarized in Table D.2.

Electrical System

All electrical switches and plugs are external to the reactor box. The only electrical devices located in the box are the solenoid valves, pressure and flow transducers, and CO detector, and the fluidized constant-

TABLE D.1

Estimates of Microreactor System Volumes and Room Air Renewal Rates

System Description	Quantity	Volume (m^3) or Air Renewal Rate (m^3/s)
A. Microreactor System Components		
1. 1/4-inch 316 SS tubing. 0.035-inch wall thickness	12.2 m	2.86×10^{-4}
2. 1/16-inch 316 SS tubing, 0.028-inch wall thickness	3.7 m	2.21×10^{-6}
3. 500-ml reactant and inert gas reservoir	3	1.5×10^{-3}
4. 150-ml reactant and inert gas reservoir	1	1.5×10^{-4}
5. Microreactor	1	5.63×10^{-7}
6. Estimated Microreactor System Volume (components 1 to 5)		1.94×10^{-3} m^3
B. Reactor Box Volume		4.08 m^3
C. Reactor Laboratory Volume		84.53 m^3
D. Air Renewal Rates		
1. Reactor Box		9.91×10^{-2} m^3/s
2. Reactor Laboratory		9.46×10^{-3} m^3/s

TABLE D.2

Upper Limits of Operating Temperatures and Pressures for Different Components of the Vibrofluidized Microreactor System

Component	Maximum Working Pressure at 21°C (kPa)	Maximum Working Pressure (kPa) at Selected Temperature
1. High pressure air regulators	17,175	
2. Stainless-steel tubing, 1/4-inch O.D.	40,574	37,325 at 315°C
3. Whitey 1/4-inch ball values	20,610	
4. Whitey sample cylinders	12,366	
5. Nupro check values	20,610	
6. Circle seal 2-way and 3-way solenoid valves	20,610	
7. Atkomatic solenoid valve	34,350	34,350 at 260°C
8. Nupro metering valves: 4SG 5MG	13,740 6,870	
9. Flexible stainless steel hose	18,274	47,870 at 315°C
10. Brooks mass-flow meters: 5810 5811	20,610 10,305	
11. Circle-seal back-pressure regulator	6,870	
12. Nupro filters	20,610	
13. Valco 6- and 10-port sampling valves		20,610 at 300°C (max)
14. Nupro in-line relief valves (350-600 psi adjustable)	20,610	

temperature sand-bath. On-off switches for these devices are located on the control panel outside the box. The fuse box is located adjacent to the reactor box so that in case of an emergency, all electricity can be shut off immediately.

The Circle-Seal solenoid valves are activated by 28 VDC via a Zenith Z-89 microcomputer. The Atkomatic solenoid valve is actuated by 24 VDC via the microcomputer. The pressure transducers are excited using 10 VDC; and both the mass-flow meters and CO detector require 120 VAC. The fluidized constant-temperature sand-bath uses 240 VAC.

Emergency Equipment

A Toxgard Model C carbon-monoxide detector (Mine Safety Appliances Company) is mounted inside the reactor box as a first line of defense against CO leaks. This detector continuously samples the air by diffusion and reports concentration in ppm. If the limit is reached, both visual and audible alarms are tripped. The sensor life of this unit is about one year. The unit is powered by the 120 VDC builidng supply.

One 5-pound CO_2 fire extinguisher is located approximately 15 m from the reactor box inside the coal laboratory. At the same location is a first-aid kit and an eyewash station.

A sling air mask, available for rescue in toxic environments, is located on the wall outside of Room 155, Randolph Hall. A telephone is located inside the coal laboratory. Emergency telephone numbers are as follows:

1.	Blacksburg Rescue Squad	9-911
2.	Blacksburg Fire Department	9-552-2222
3.	Campus Police	6411
4.	University Health Services	6444
5.	Montgomery County Hospital	9-951-1111

Emergency Shutdown Procedures

A. Fire Emergency

1. Turn off the main valve on the hydrogen cylinder.
2. Turn off the main valve on the H_2:CO:Ar cylinder.
3. Call Blacksburg Fire Department at 9-552-2222.
4. Notify a close-by person to sound the fire alarm and evacuate the building.
5. If fire is small and confined in nature, steps may be taken to extinguish it with the CO_2 fire extinguisher.

B. Gas Leaks

1. Turn off all electricity to the experiment at the control panel of the fuse box.
2. Turn off the main valve on the hydrogen cylinder.
3. Turn off the main valve on the H_2:CO:Ar cylinder.
4. Locate leak site using nitrogen and repair the leak.
5. Pessure-test the system after leak repair.

C. Loss of Building Power

1. Turn off the main valve on the H_2:CO:Ar cylinder.
2. Turn off the main valve on the hydrogen cylinder.
3. Turn off the main valve on the nitrogen cylinder.
4. Turn off all meters and solenoid valves.
5. Wait for power restoration in another room.

APPENDIX E

EARLIER EXPLORATORY WORK

The development of the present unsteady-state microreactor system for F-T synthesis has taken place over a three-year period. During this time, the design of the microreactor system as well as the microreactor itself has been revised several times.

Figures E.1 and E.2 are photographs of the original stainless-steel vibrofluidized microreactor used in preliminary experiments (Liu et al., 1982). This microreactor consisted of four primary zones: (1) the plenum zone, (2) the reaction zone, (3) the freeboard zone and (4) the product-gas exit zone. The internal dimensions of the microreactor were very similar to those of the steady-state microreactor shown in Figure 4.2. Asbestos impregnated gaskets were used between the four sections of the microreactor. This is in contrast to the silver-plated stainless-steel O-rings now being used in the present reactor. The use of gaskets coupled with the lack of compressive force exerted by the four connecting bolts, resulted in gas leakage at the high temperatures and pressures used. Leakage also occurred at silver-soldered tubing joints which tended to soften at high temperature. In the present microreactor, all tubing joints have been welded for leak-proof seals.

Figure E.3 is a schematic diagram of the original design of the vibrofluidized-bed microreactor system for unsteady-state F-T synthesis. This system consisted of two feed legs, a product-exit leg and a purge gas-exit leg. The idea was to provide discrete pulses of gas to the catalyst bed by alternately purging the plenum zone of the previous gas. Figures E.4 through E.8 illustrate the feeding and purging sequence:

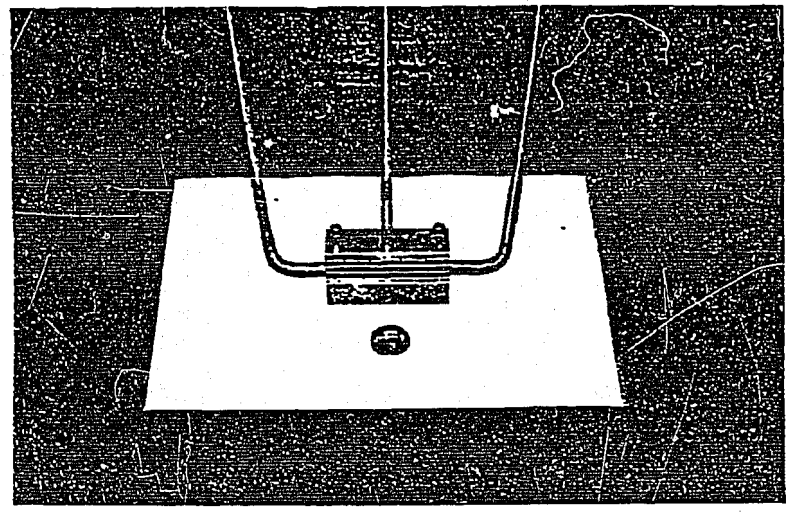

Figure E.1. The Original Vibrofluidized Microreactor for Fischer-Tropsch Synthesis Studies.

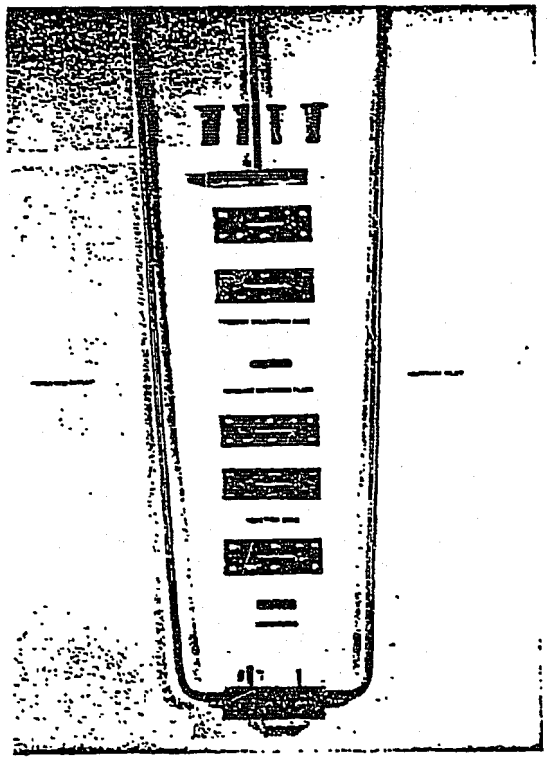

Figure E.2. Key Components of the Vibrofluidized Microreactor for Fischer-Tropsch Synthesis Studies.

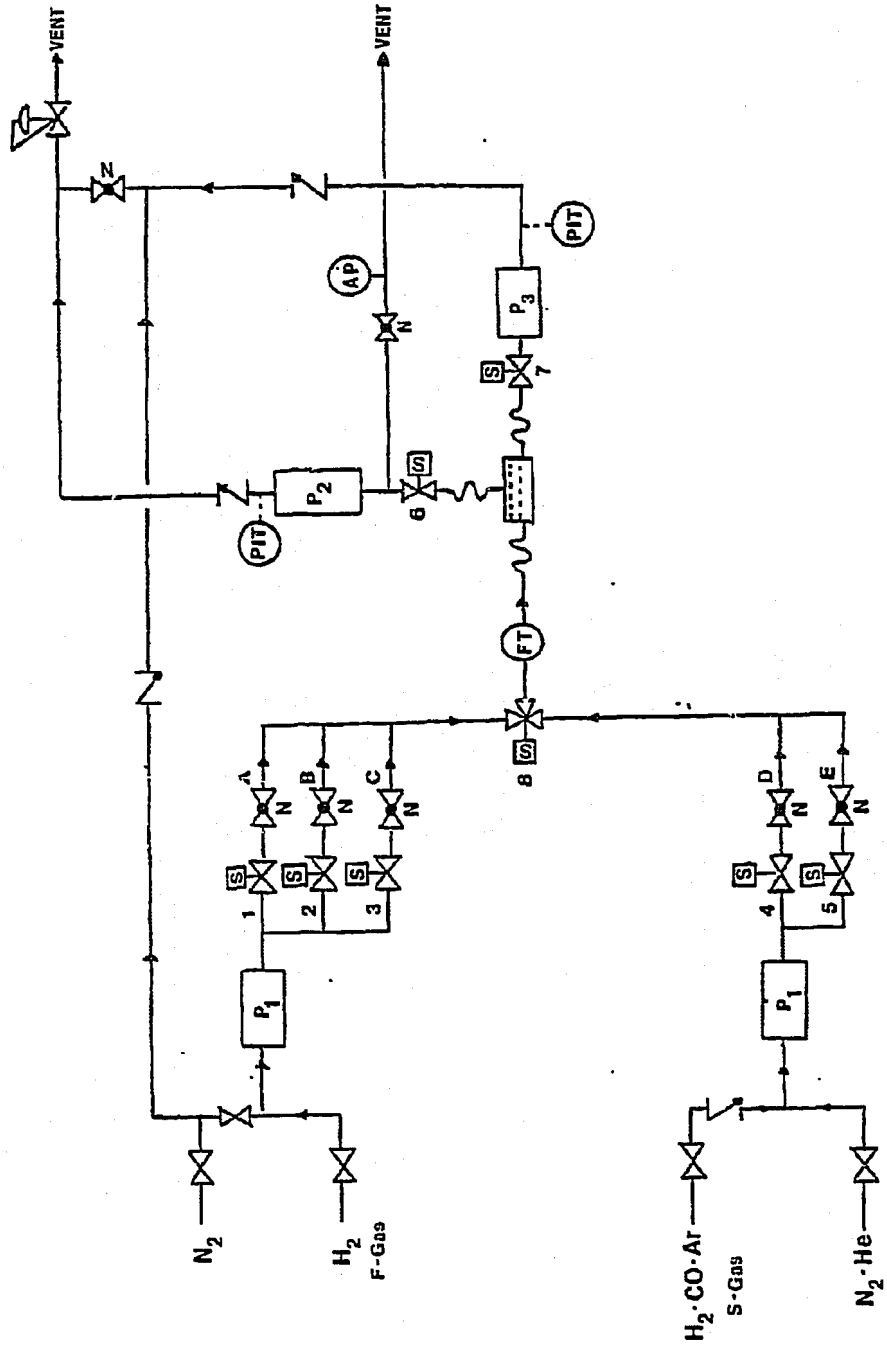

Figure E.3. A Schematic Diagram of the Original Vibrofluidized-Bed Microreactor System for Unsteady-State Fischer-Tropsch Synthesis (Refer to Figure 4.1b for Equipment Symbols).

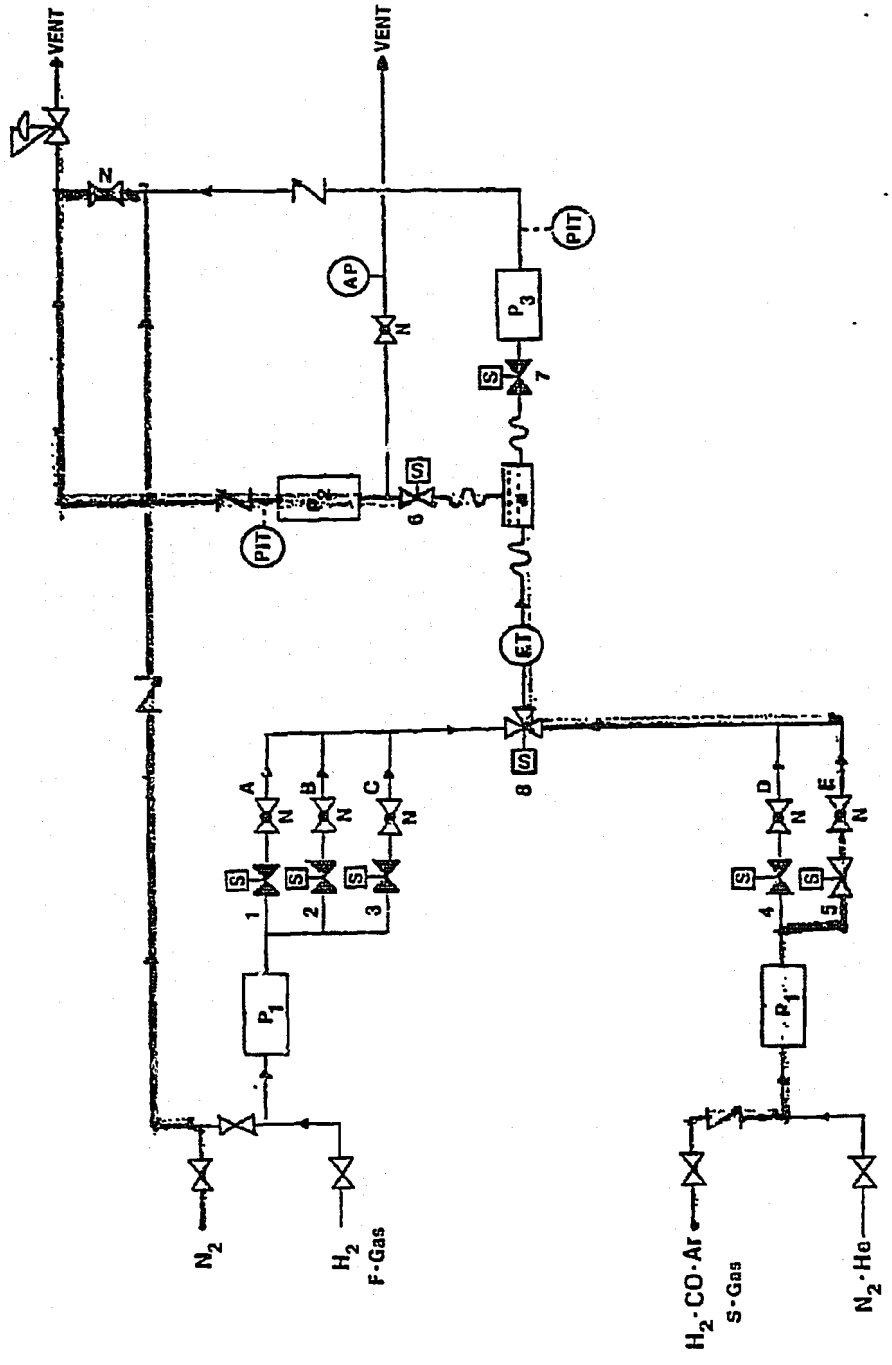

Figure E.4. High Flow Rate of S-Gas Feed through Valve E for a Short Duration.

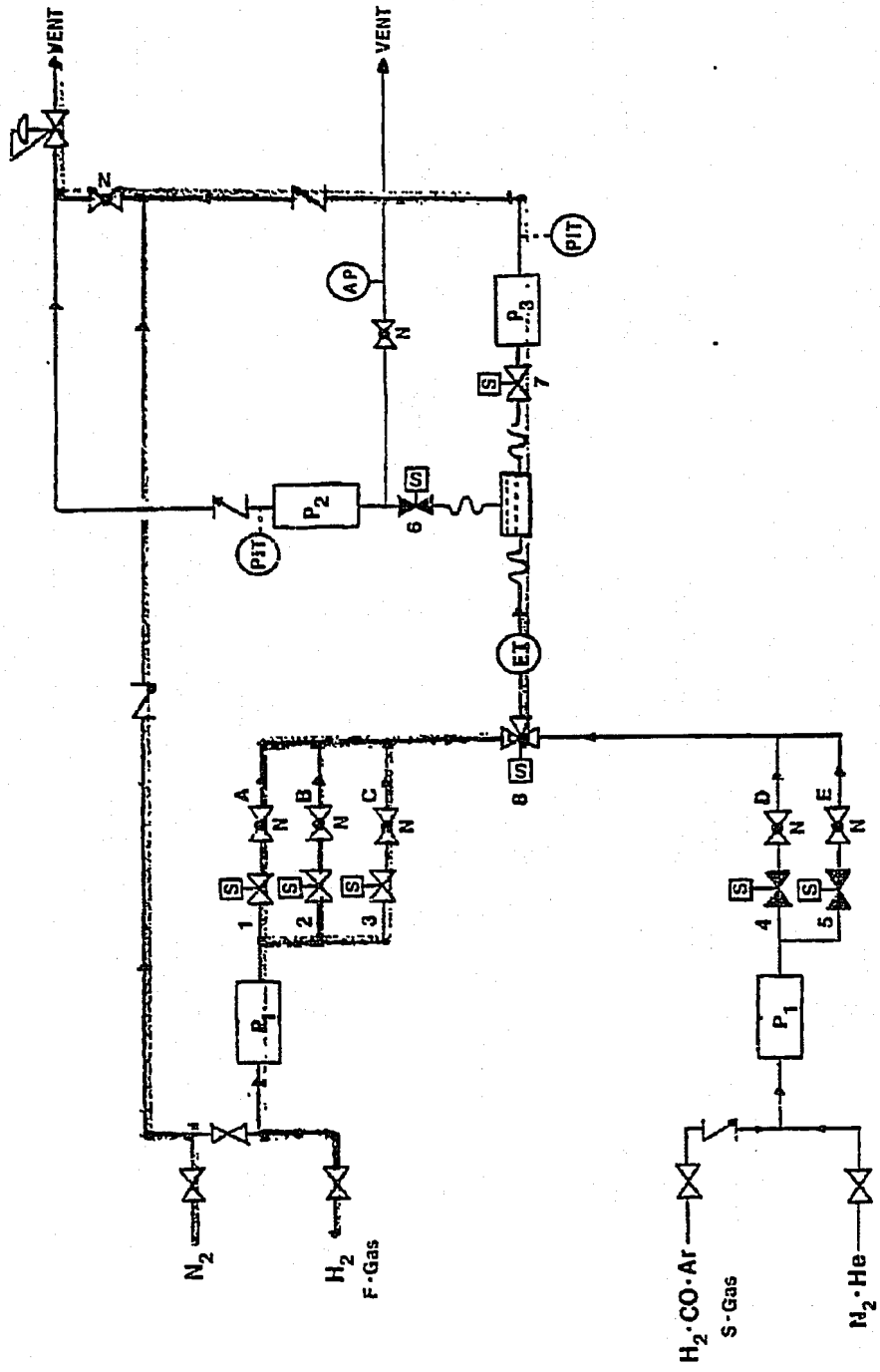

Figure E.5. Plenum Purge of S-Gas by a High Flow Rate of F-Gas for a Short Duration.

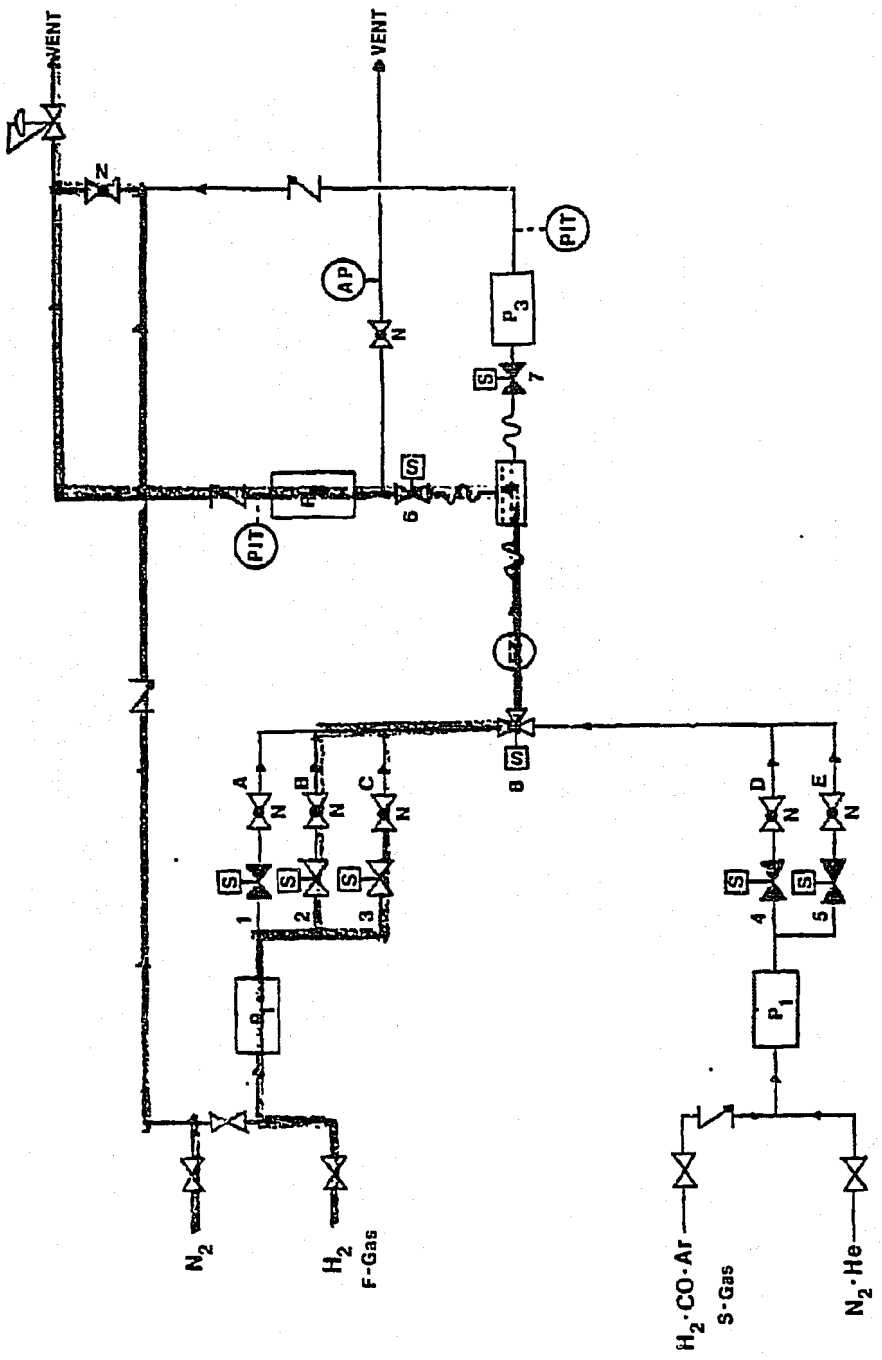

Figure E.6. Reaction Zone Purge by a Relatively High Flow Rate of F-Gas for a Short Duration.

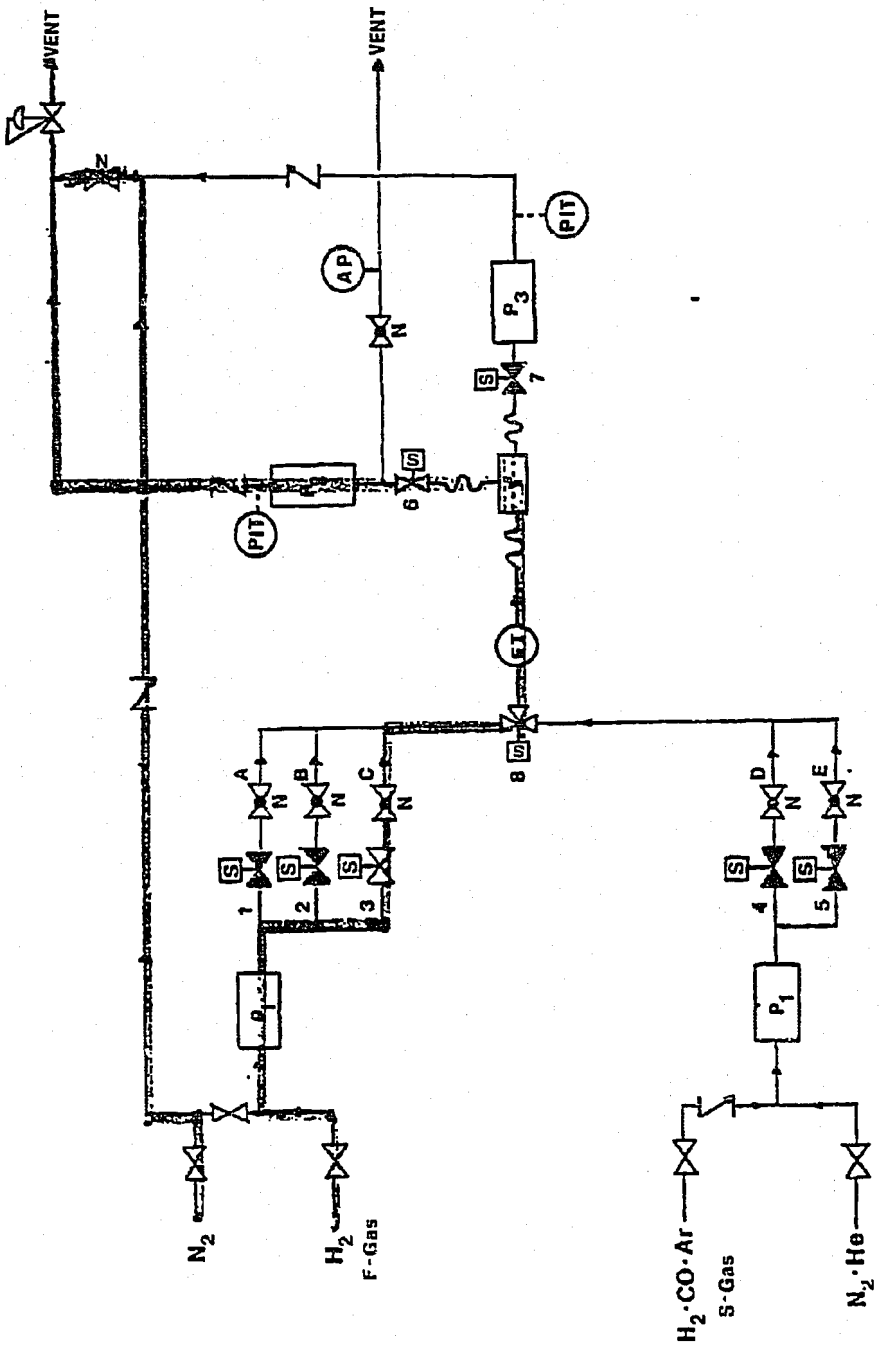

Figure E.7. A Low Flow Rate of F-Gas Feed into the Reaction Zone through Valve C for a Long Duration.

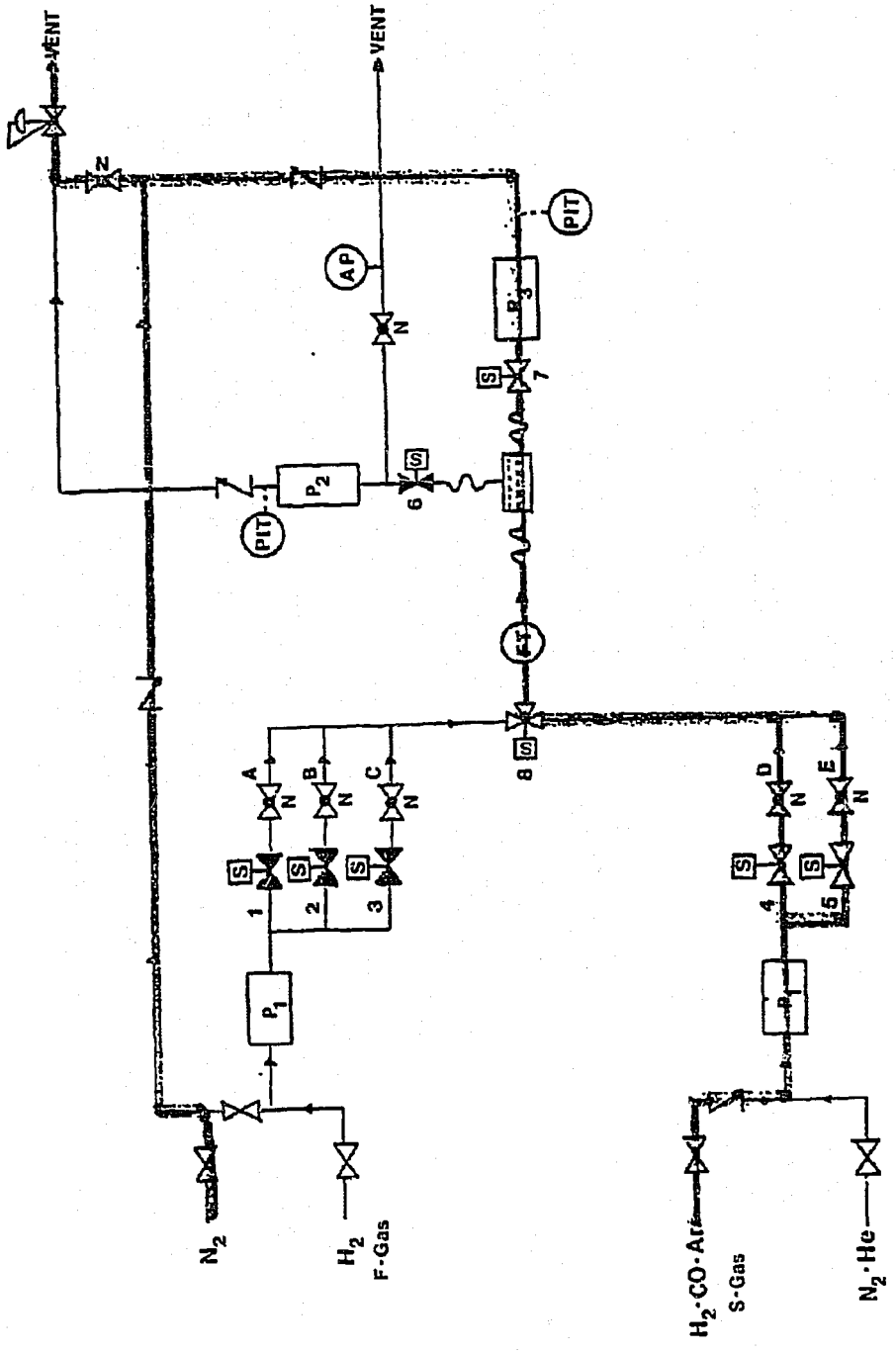

Figure E.8. Plenum Purge of F-Gas by a High Flow Rate of S-gas for a Short Duration.

(i) S-gas (H_2:CO:Ar) is being fed at the beginning of a cycle (Figure E.4). Solenoid valves 1, 2, 3, 4, and 7 are closed. Three-way solenoid valve 8 is shifted to permit a high flow rate of S-gas into the microreactor for a short duration (e.g., 2 seconds).

(ii) The plenum zone beneath the catalyst zone is being purged of S-gas by F-gas (Figure E.5). Solenoid valves 4, 5, and 6 are closed and three-way valve 8 is shifted to permit the F-gas to flow. At this time, solenoid valves 1, 2, 3, and 7 are opened simultaneously for a relatively high flow rate of F-gas through needle valves A, B, and C into the plenum zone of the microreactor for a short duration (e.g., 1 second). This flow should be able to purge the gas contained in the plenum zone completely.

(iii) The reaction zone is being purged by F-gas (Figure E.6). Solenoid valve 1 and 7 are closed and 6 is opened. This permits a relatively high flow rate of F-gas through needle valves B and C for a short duration (e.g., 1 second).

(iv) F-gas is being fed into the reaction zone (Figure E.7). Valve 2 is closed and valves 3 and 6 remain open. A low flow rate of F-gas passes through valves 3 and C into the reaction zone for a long duration.

(v) The plenum zone is being purged of F-gas by S-gas (Figure E.8). Valves 3 and 6 are closed, and valves 4, 5, and 7 remain open. Three-way value 8 is shifted to its original position which allows for the S-gas to flow into the plenum zone through valves D and E at a high flow rate for a very short duration. This flow should be able to sweep-out the gas contained in the plenum zone in the microreactor.

After several preliminary experiments, a cold-flow model of the unsteady-state microreactor system was constructed. The purpose of this model was to determine the gas-mixing characteristics of the microreactor system. The results of the earlier cold-flow model studies have been given by Feldhousen (1984). It was found that undesirable mixing of F-gas and S-gas occurred in the plenum zone of the microreactor. In addition, it has been suggested that the plenum purge period provided an "aging" time for the catalyst during which no gas was flowing through the catalyst bed.

Because of these results, the sliding-plug vibrofluidized-bed microreactor system described in Sections 5 and 6 has been developed. The sliding-plug vibrofluidized-bed microreactor system drastically reduces gas mixing and allows the catalyst to be continually exposed to gas flow.

APPENDIX F

Thermal Conductivity Detector Traces of Gas Mixing in the Sliding-Plug Vibrofluidized-Bed Cold-Flow Microreactor Model

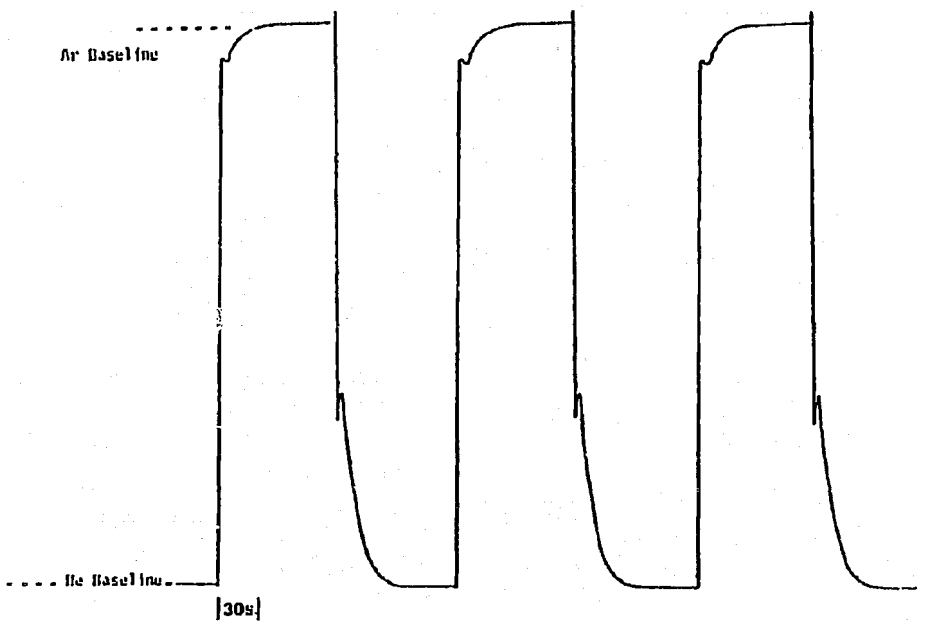

Figure F.1. The Thermal Conductivity Response for Switching Between Helium and Argon Feeds in the Cold-Flow Microreactor Model during Experiment 1-1. (Refer to Table 5.1 for the Experimental Conditions).

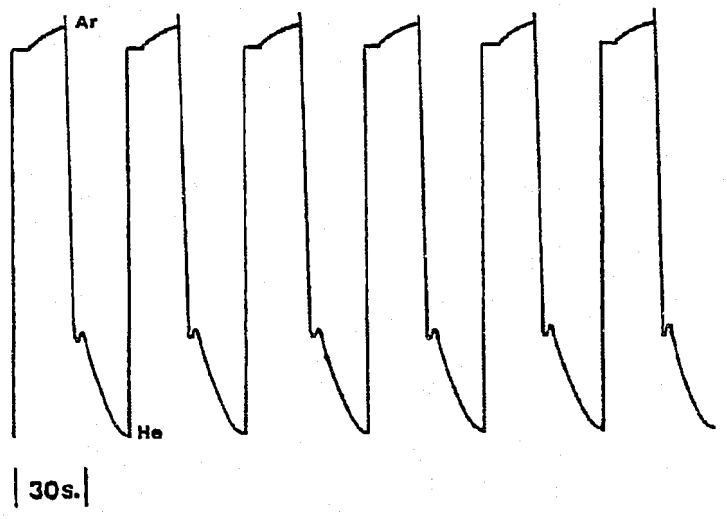

Figure F.2. The Thermal Conductivity Response for Switching Between Helium and Argon Feeds in the Cold-Flow Microreactor Model during Experiment 1-2 (Refer to Table 5.1 for the Experimental Conditions).

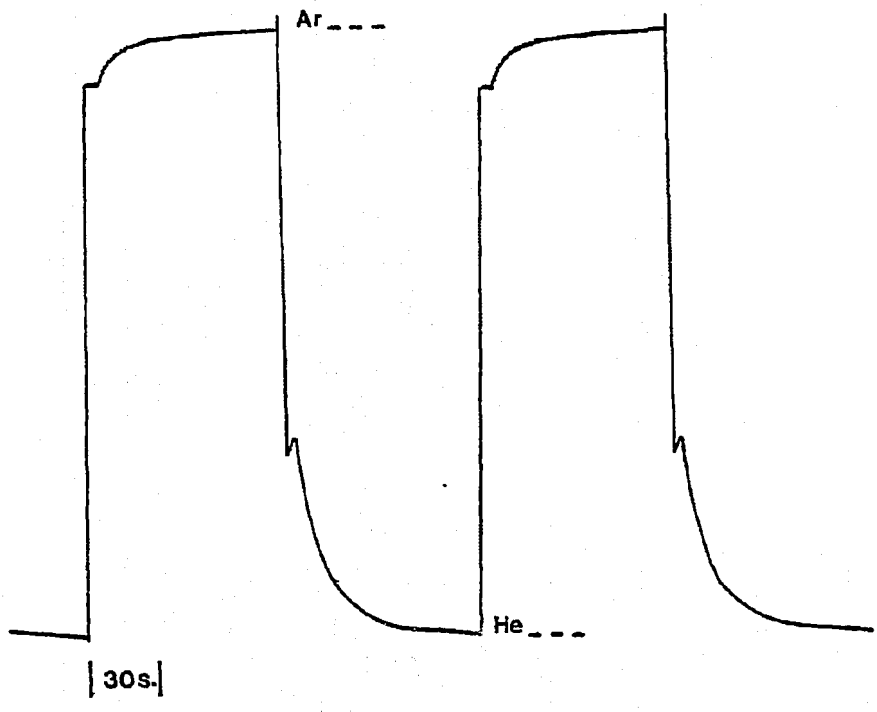

Figure F.3. The Thermal Conductivity Response for Switching Between Helium and Argon Feeds in the Cold-Flow Microreactor Model during Experiment 1-4 (Refer to Table 5.1 for the Experimental Conditions).

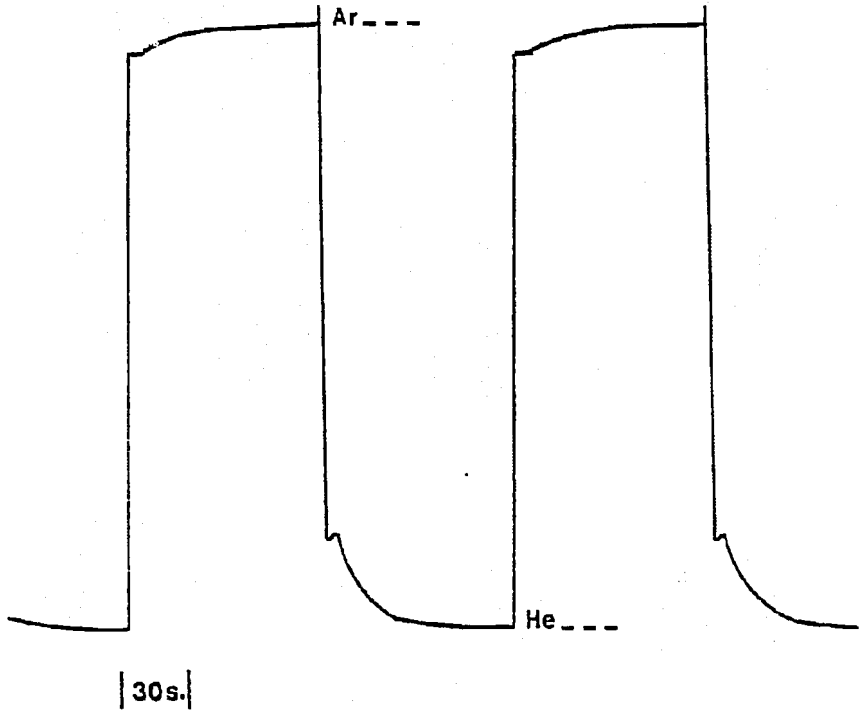

Figure F.4. The Thermal Conductivity Response for Switching Between Helium and Argon Feeds in the Cold-Flow Microreactor Model during Experiment 1-5 (Refer to Table 5.1 for the Experimental Conditions).

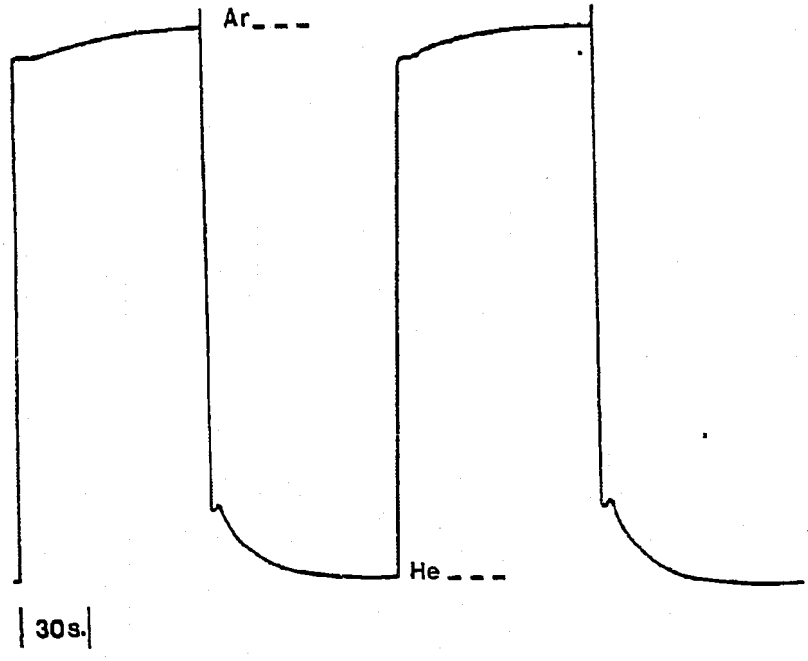

Figure F.5. The Thermal Conductivity Response for Switching Between Helium and Argon Feeds in the Cold-Flow Microreactor Model during Experiment 1-6 (Refer to Table 5.1 for the Experimental Conditions).

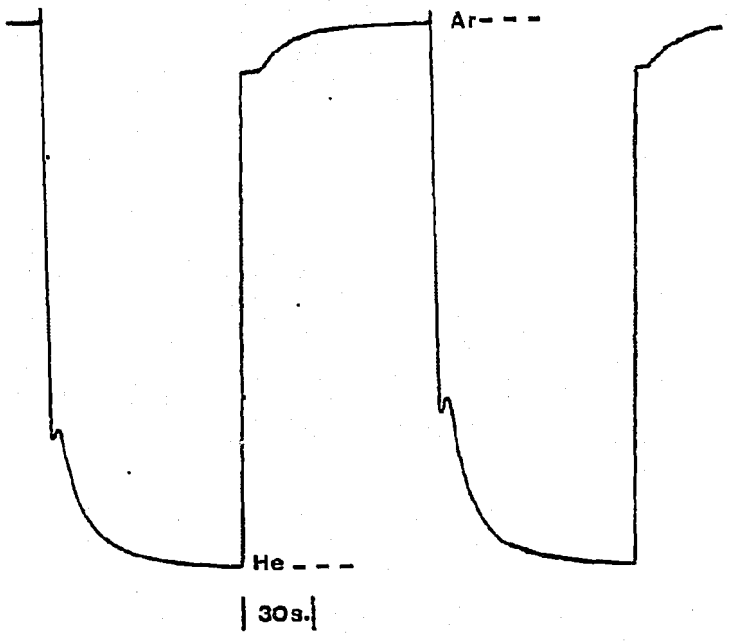

Figure F.6. The Thermal Conductivity Response for Switching Between Helium and Argon Feeds in the Cold-Flow Microreactor Model during Experiment 1-7 (Refer to Table 5.1 for the Experimental Conditions).

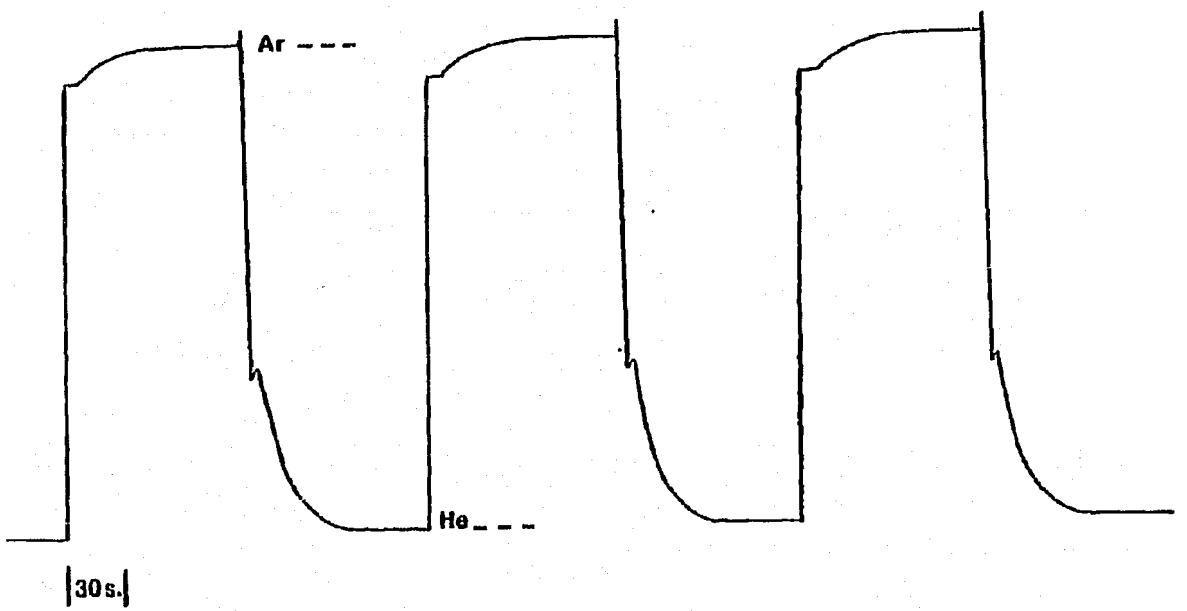

Figure F.7. The Thermal Conductivity Response for Switching Between Helium and Argon Feeds in the Cold-Flow Microreactor Model during Experiment 1-8 (Refer to Table 5.1 for the Experimental Conditions).

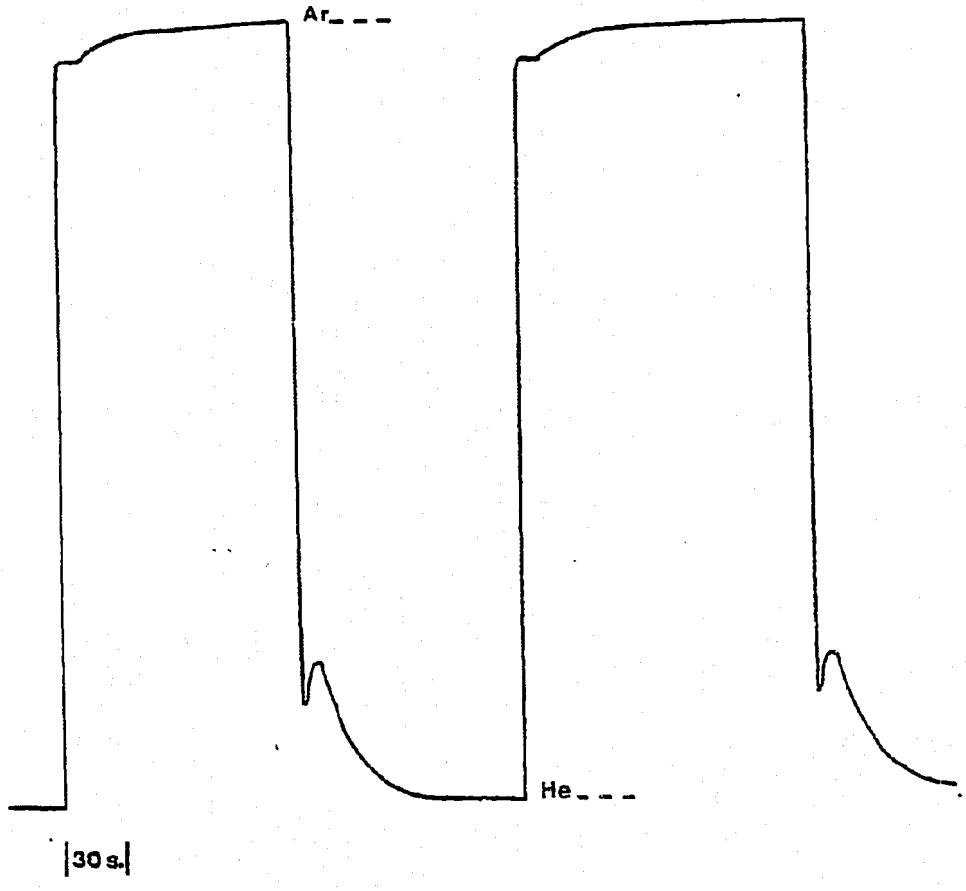

Figure F.8. The Thermal Conductivity Response for Switching Between Helium and Argon Feeds in the Cold-Flow Microreactor Model during Experiment 2-1 (Refer to Table 5.1 for the Experimental Conditions).

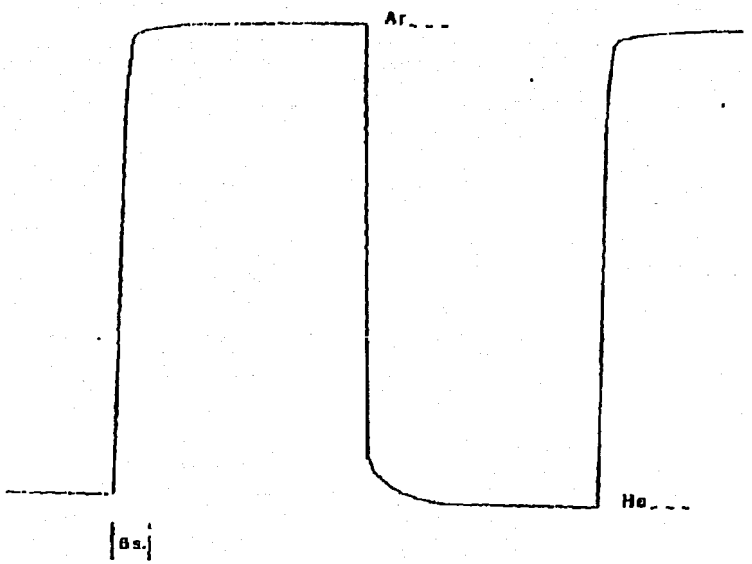

Figure F.9. The Thermal Conductivity Response for Switching Between Helium and Argon Feeds in the Cold-Flow Microreactor Model during Experiment 2-3 (Refer to Table 5.1 for the Experimental Conditions).

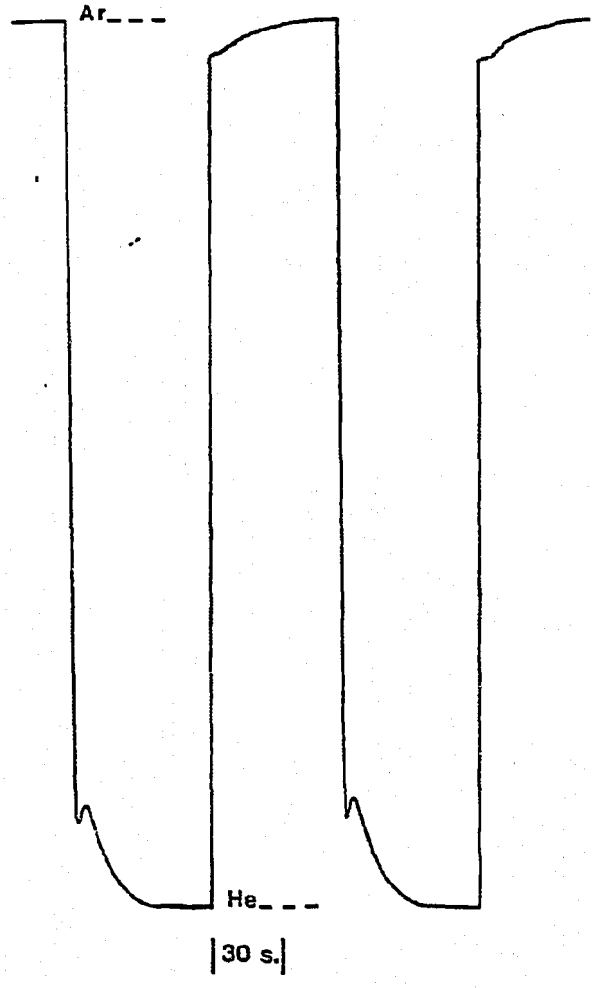

Figure F.10. The Thermal Conductivity Response for Switching Between Helium and Argon Feeds in the Cold-Flow Microreactor Model during Experiment 2-4 (Refer to Table 5.1 for the Experimental Conditions).

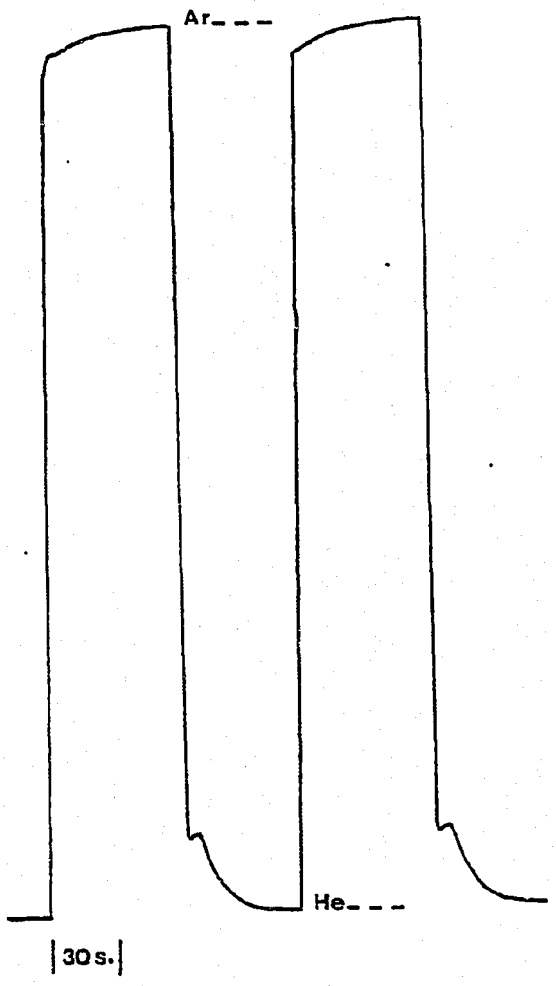

Figure F.11. The Thermal Conductivity Response for Switching Between Helium and Argon Feeds in the Cold-Flow Microreactor Model during Experiment 2-5 (Refer to Table 5.1 for the Experimental Conditions).

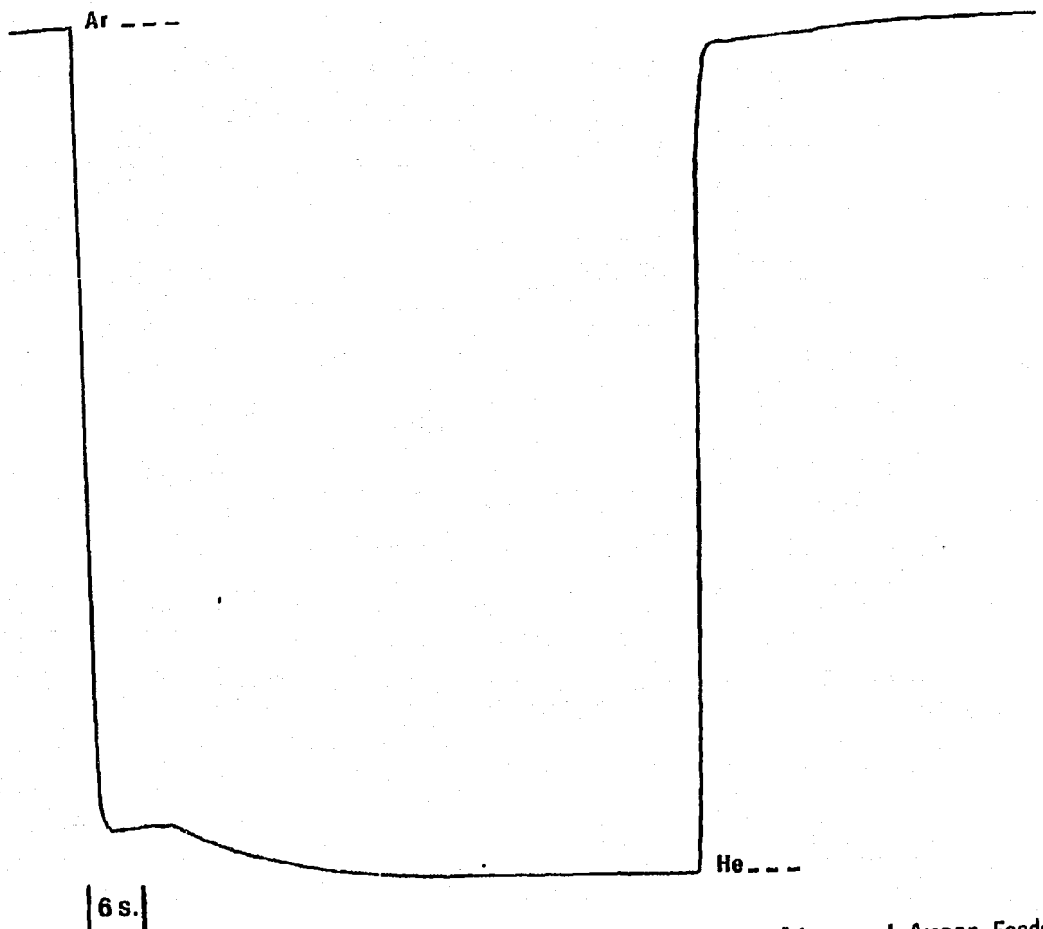

Figure F.12. The Thermal Conductivity Response for Switching Between Helium and Argon Feeds in the Cold-Flow Microreactor Model during Experiment 2-6 (Refer to Table 5.1 for the Experimental Conditions).

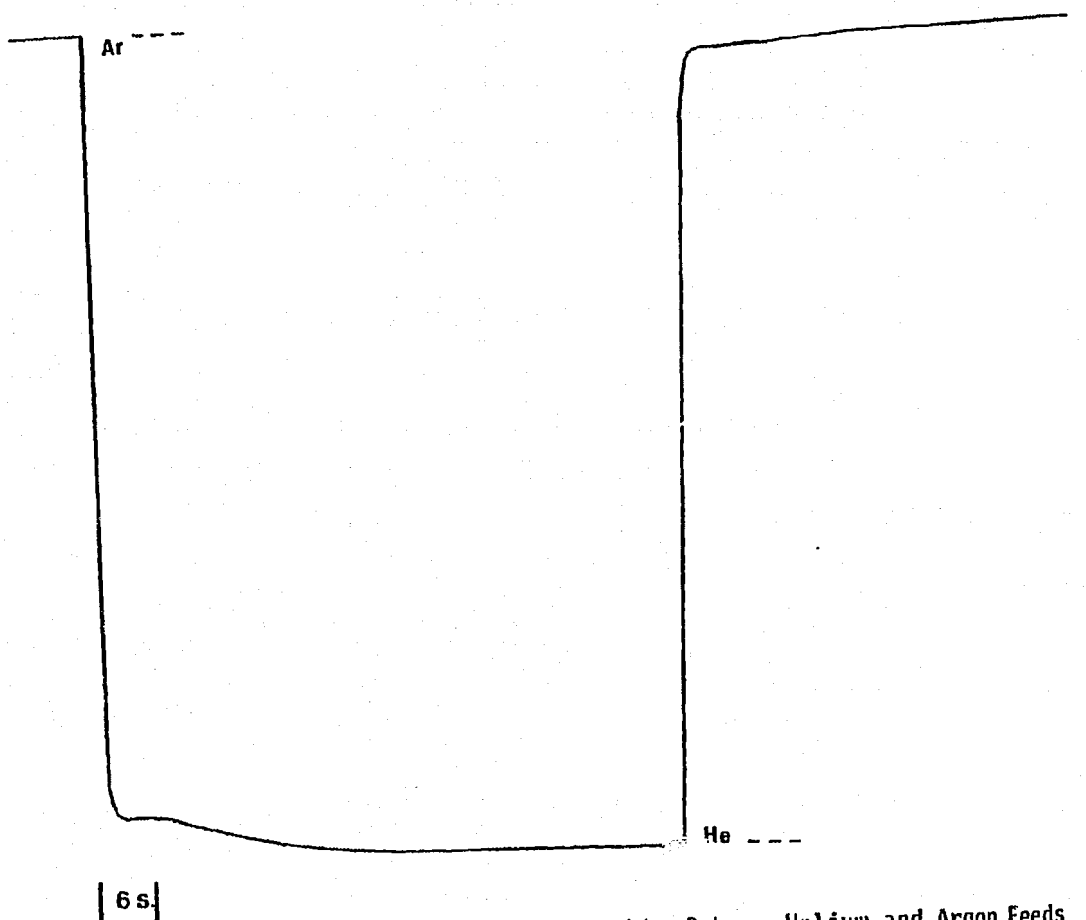

Figure F.13. The Thermal Conductivity Response for Switching Between Helium and Argon Feeds in the Cold-Flow Microreactor Model during Experiment 2-7 (Refer to Table 5.1 for the Experimental Conditions).

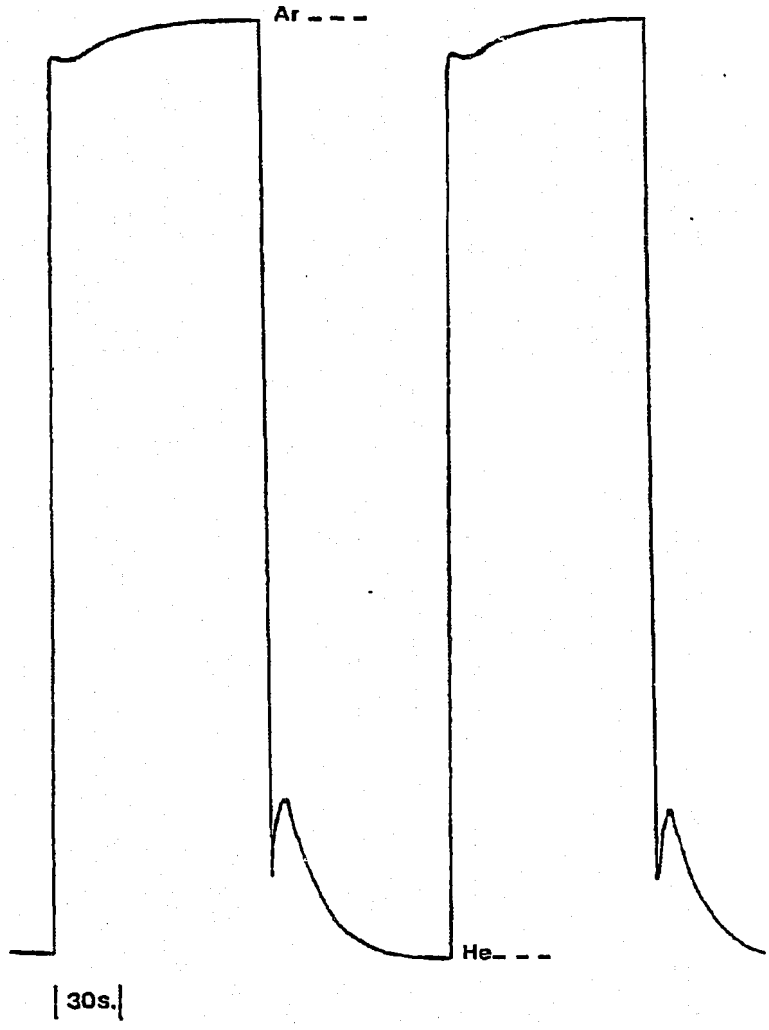

Figure F.14. The Thermal Conductivity Response for Switching Between Helium and Argon Feeds in the Cold-Flow Microreactor Model during Experiment 2-8 (Refer to Table 5.1 for the Experimental Conditions).

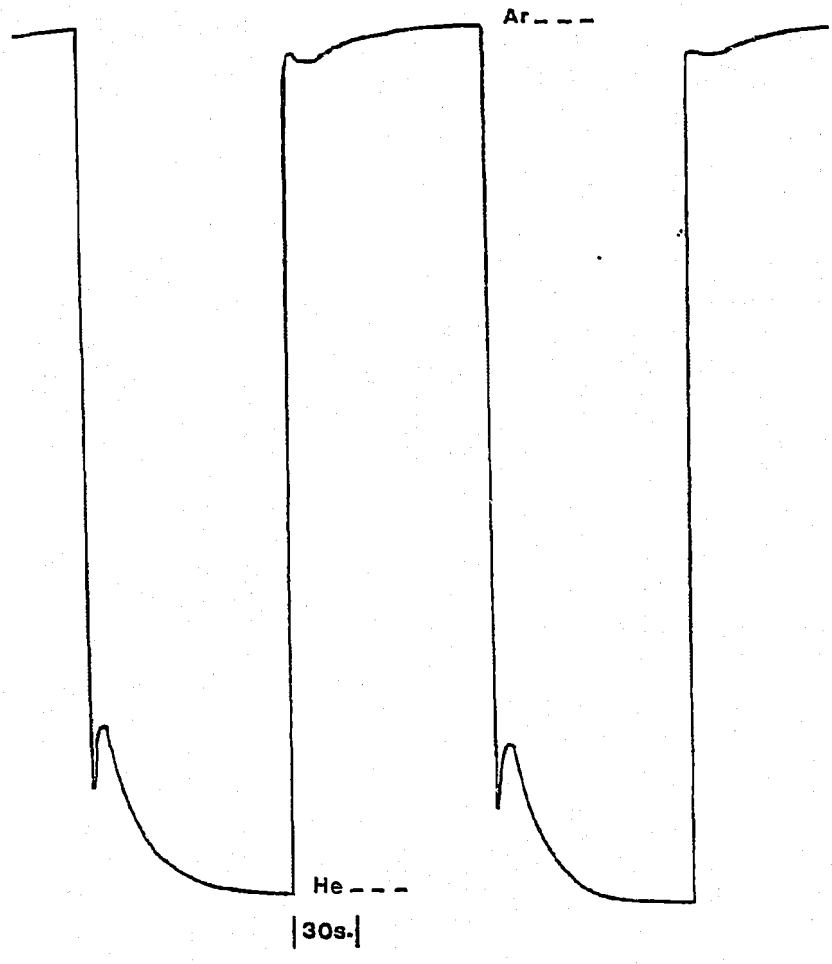

Figure F.15. The Thermal Conductivity Response for Switching Between Helium and Argon Feeds in the Cold-Flow Microreactor Model during Experiment 2-9 (Refer to Table 5.1 for the Experimental Conditions).

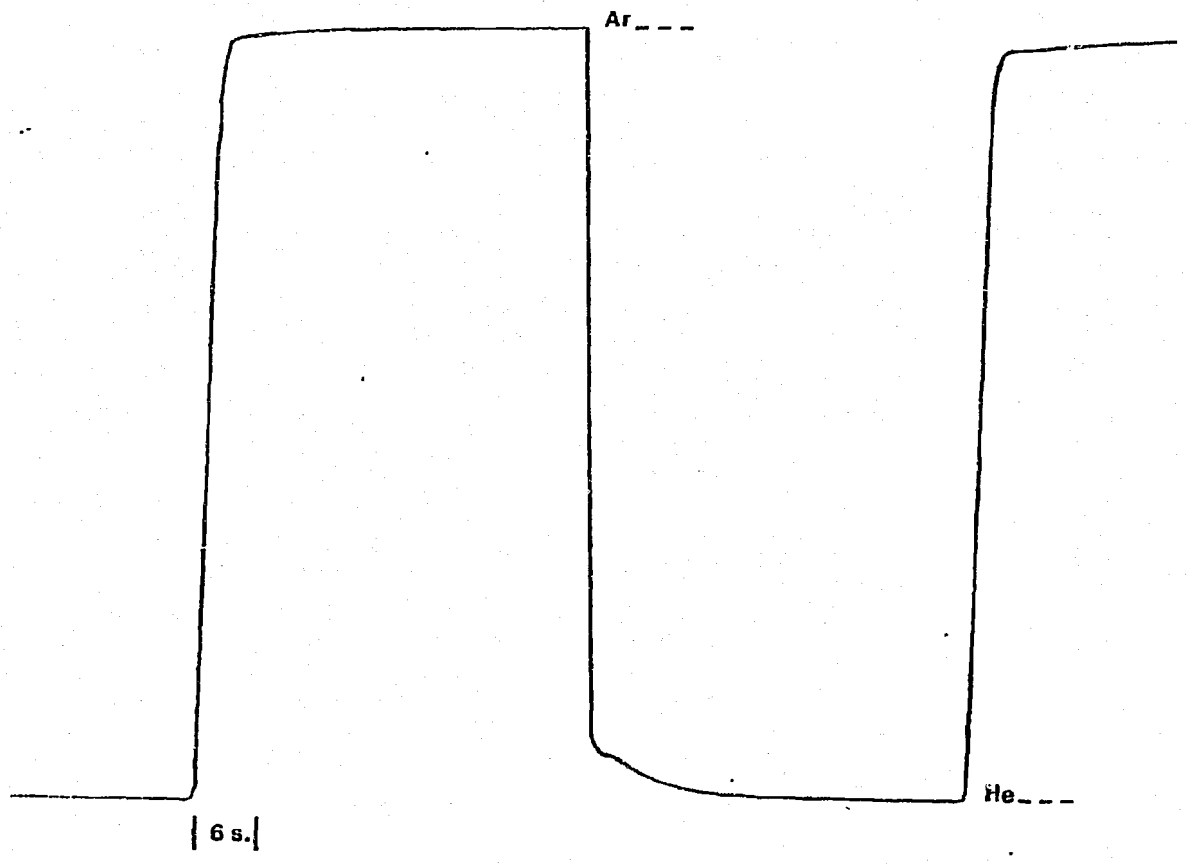

Figure F.16. The Thermal Conductivity Response for Switching Between Helium and Argon Feeds in the Cold-Flow Microreactor Model during Experiment 2-10 (Refer to Table 5.1 for the Experimental Conditions).

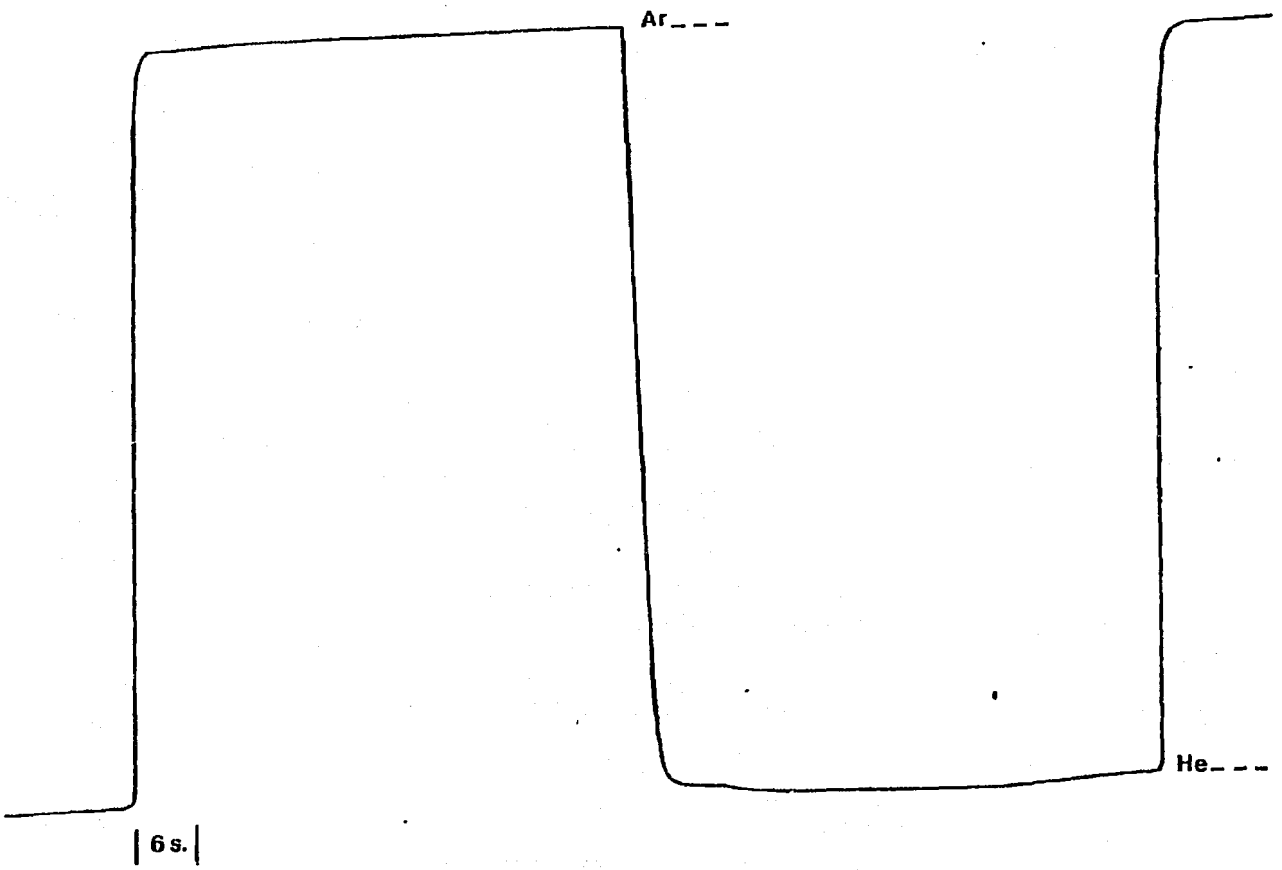

Figure F.17. The Thermal Conductivity Response for Switching Between Helium and Argon Feeds in the Cold-Flow Microreactor Model during Experiment 2-11 (Refer to Table 5.1 for the Experimental Conditions).

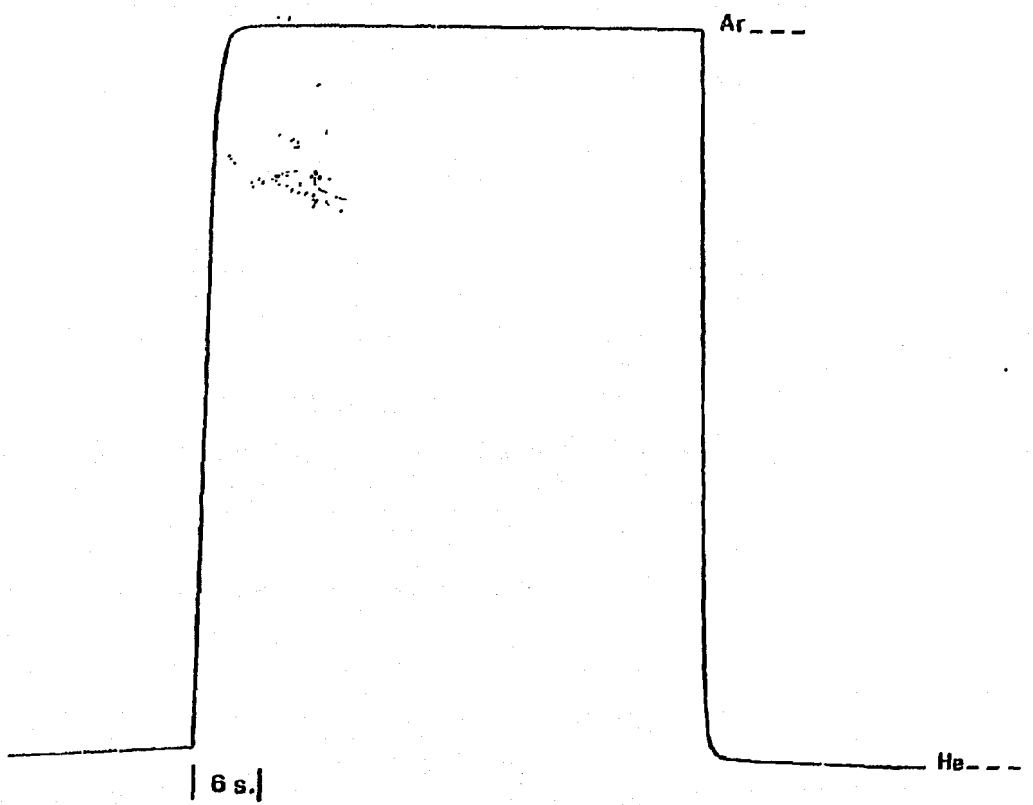

Figure F.18. The Thermal Conductivity Response for Switching Between Helium and Argon Feeds in the Cold-Flow Microreactor Model during Experiment 2-13 (Refer to Table 5.1 for the Experimental Conditions).

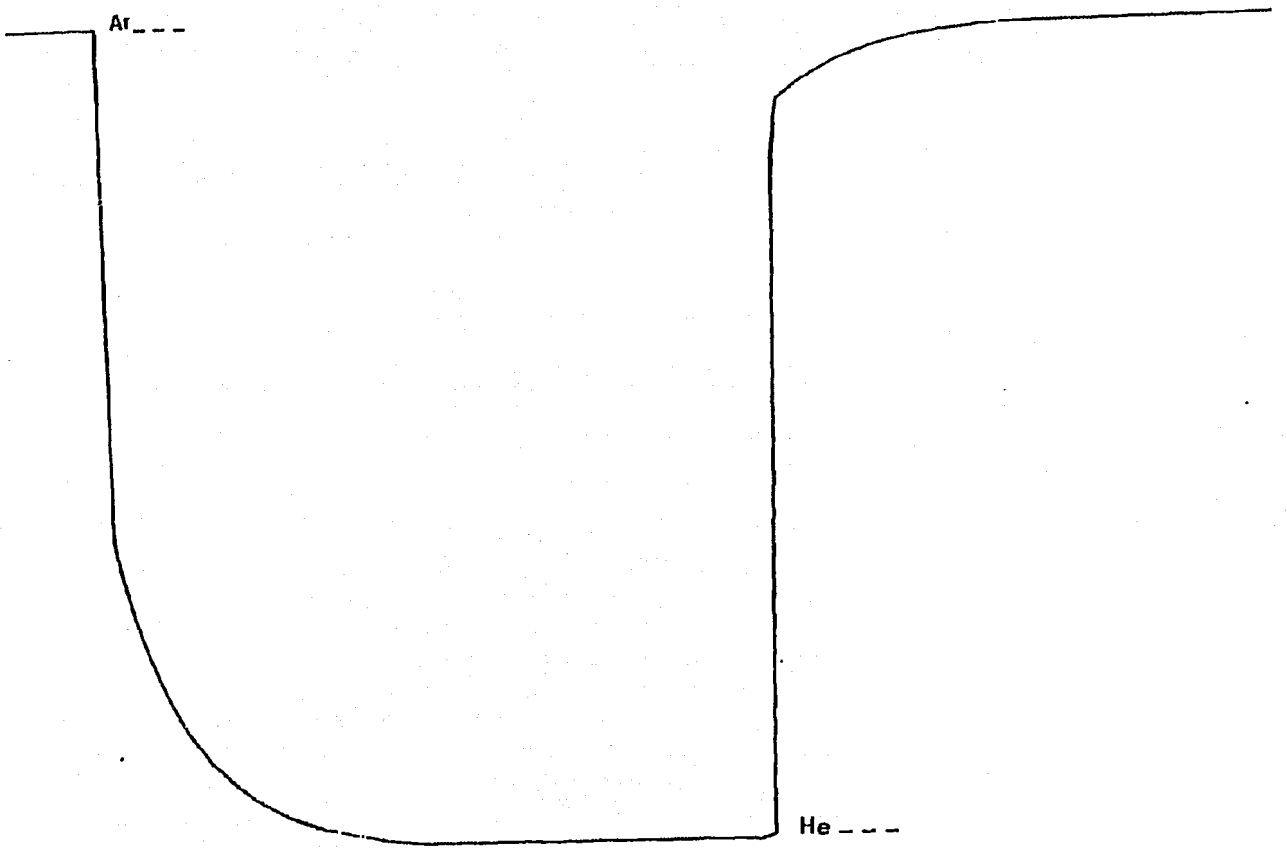

Figure F.19. The Thermal Conductivity Response for Switching Between Helium and Argon Feeds in the Cold-Flow Microreactor Model during Experiment 3-1 (Refer to Table 5.1 for the Experimental Conditions).

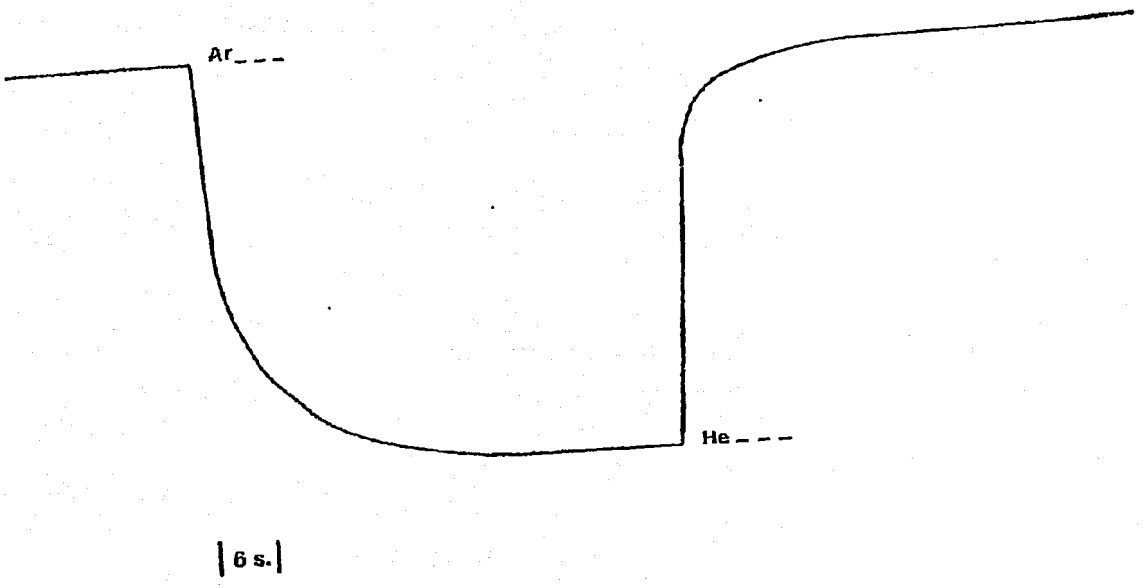

Figure F.20. The Thermal Conductivity Response for Switching Between Helium and Argon Feeds. in the Cold-Flow Microreactor Model during Experiment 3-2 (Refer to Table 5.1 for the Experimental Conditions).

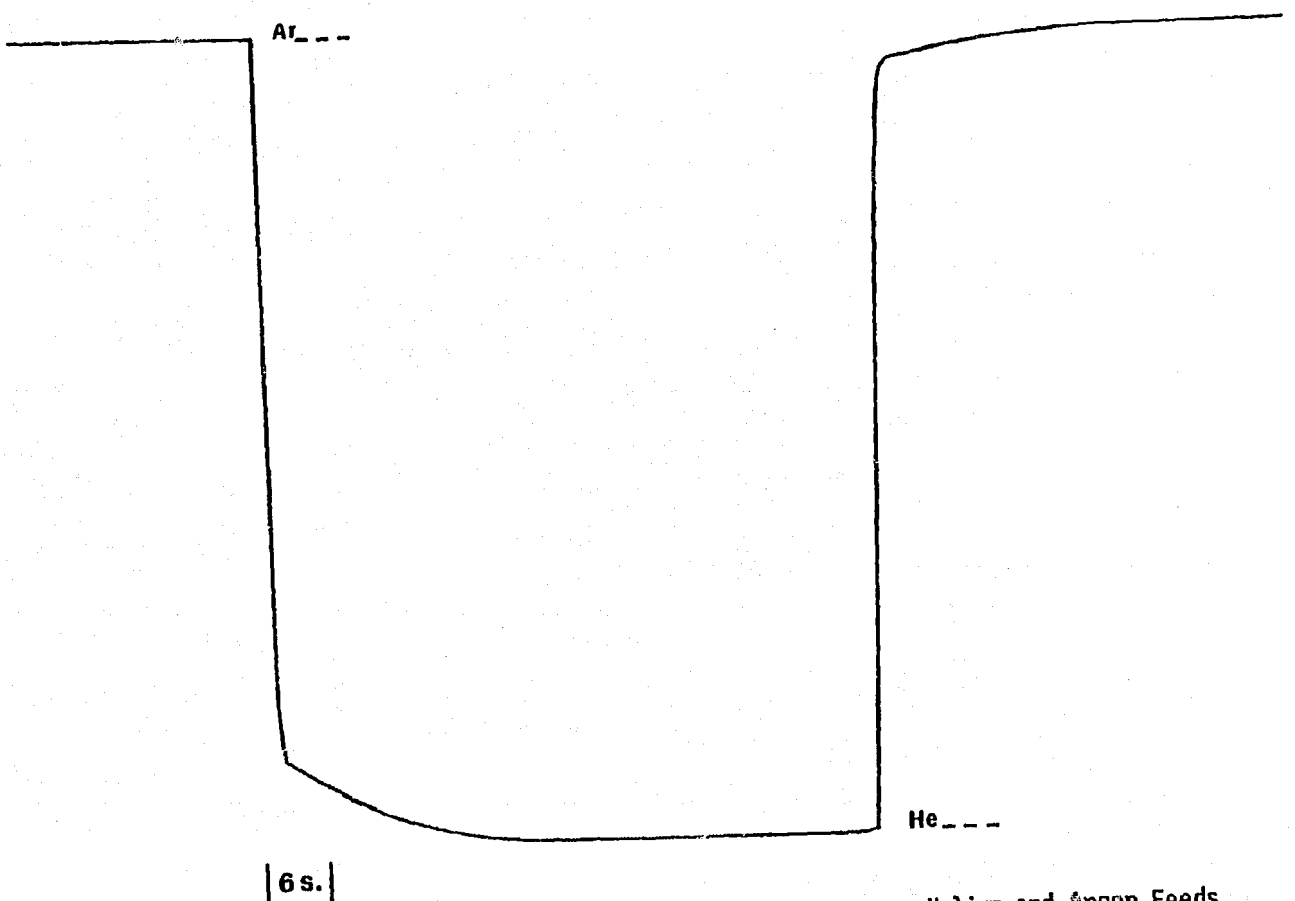

Figure F.21. The Thermal Conductivity Response for Switching Between Helium and Argon Feeds in the Cold-Flow Microreactor Model during Experiment 3-3 (Refer to Table 5.1 for the Experimental Conditions).

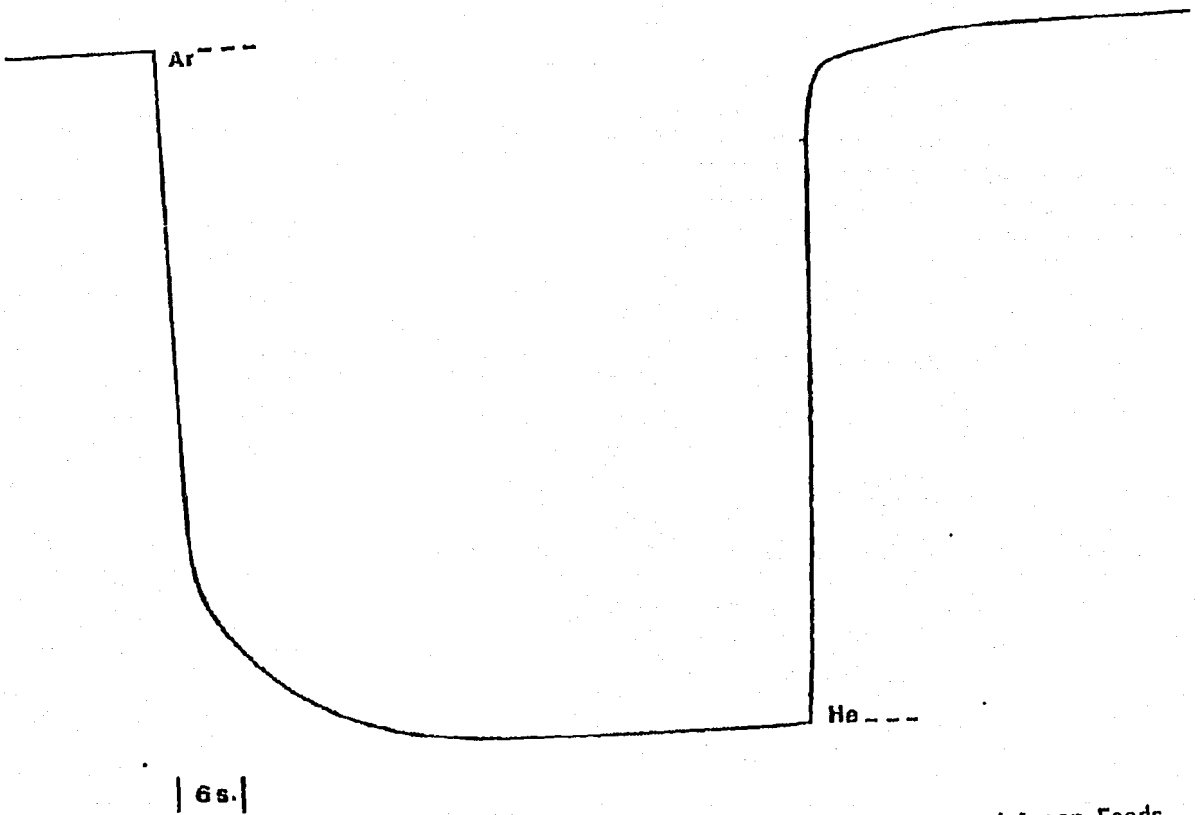

Figure F.22. The Thermal Conductivity Response for Switching Between Helium and Argon Feeds in the Cold-Flow Microreactor Model during Experiment 3-4 (Refer to Table 5.1 for the Experimental Conditions).

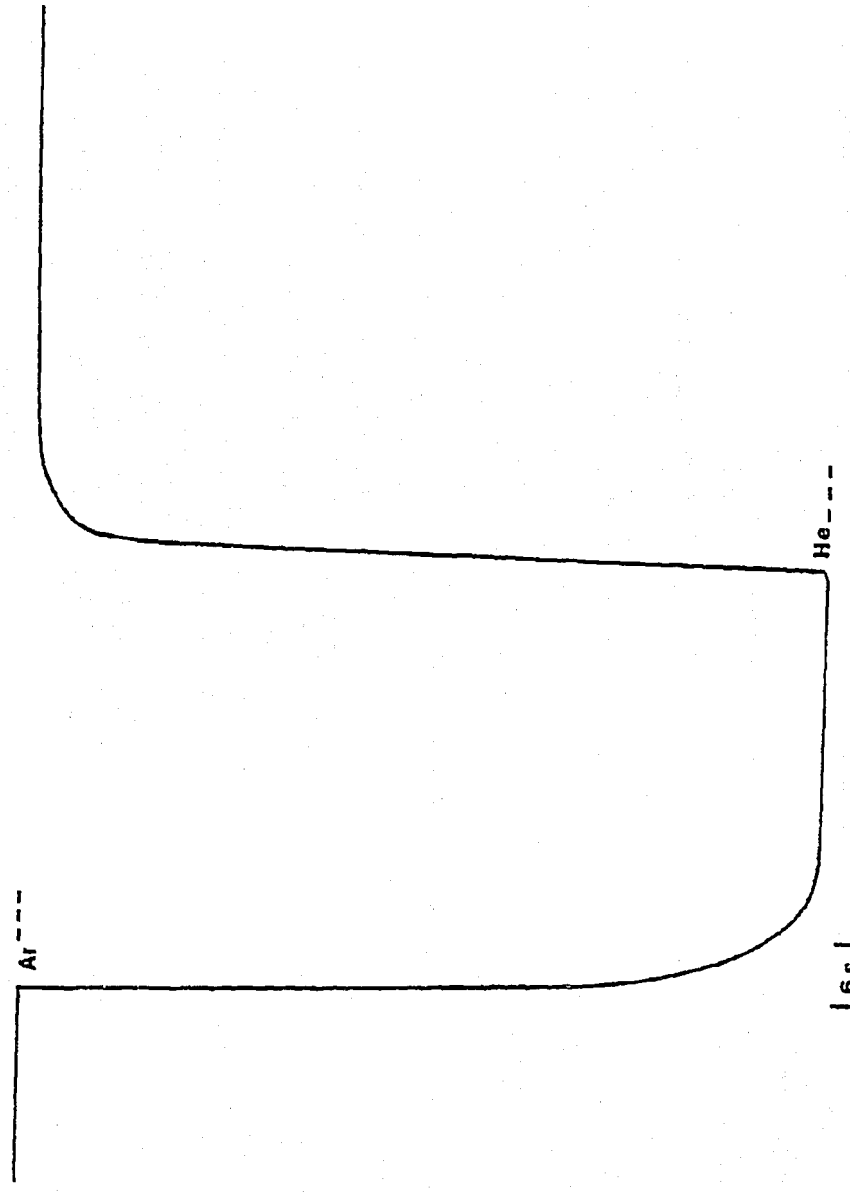

Figure F.23. The Thermal Conductivity Response for Switching Between Helium and Argon Feeds in the Cold-Flow Microreactor Model during Experiment 3-5 (Refer to Table 5.1 for the Experimental Conditions).

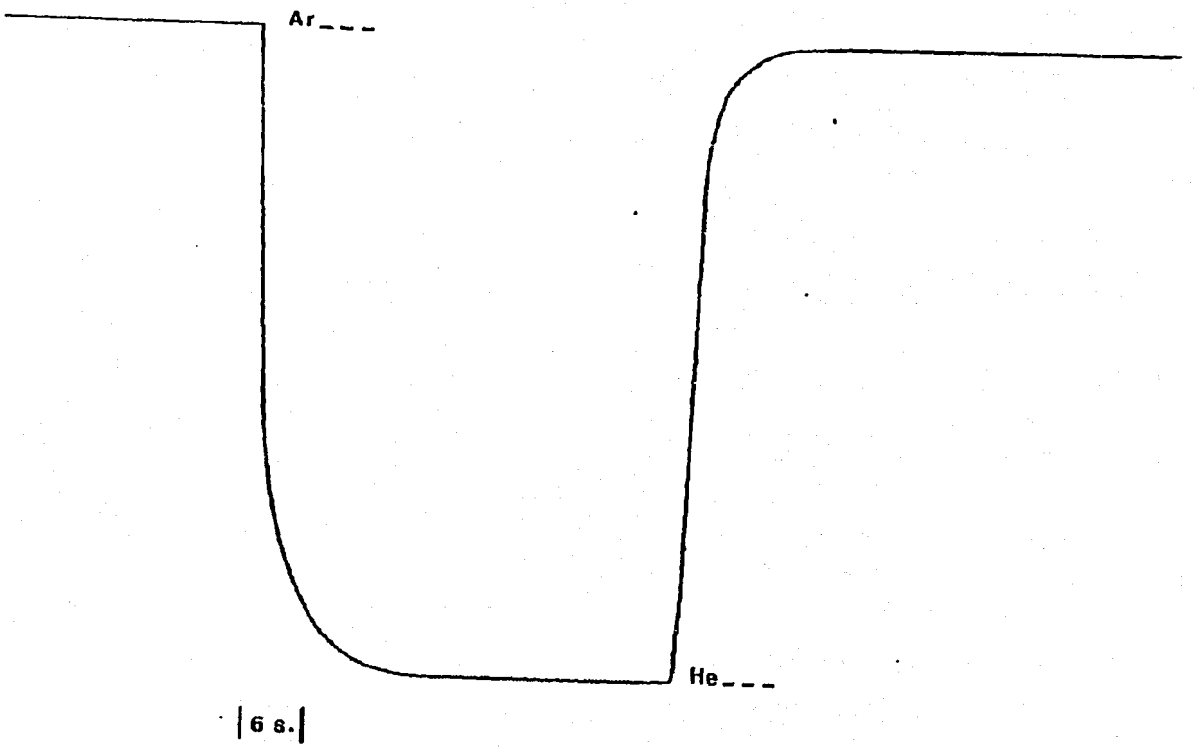

Figure F.24. The Thermal Conductivity Response for Switching Between Helium and Argon Feeds in the Cold-Flow Microreactor Model during Experiment 3-6 (Refer to Table 5.1 for the Experimental Conditions).

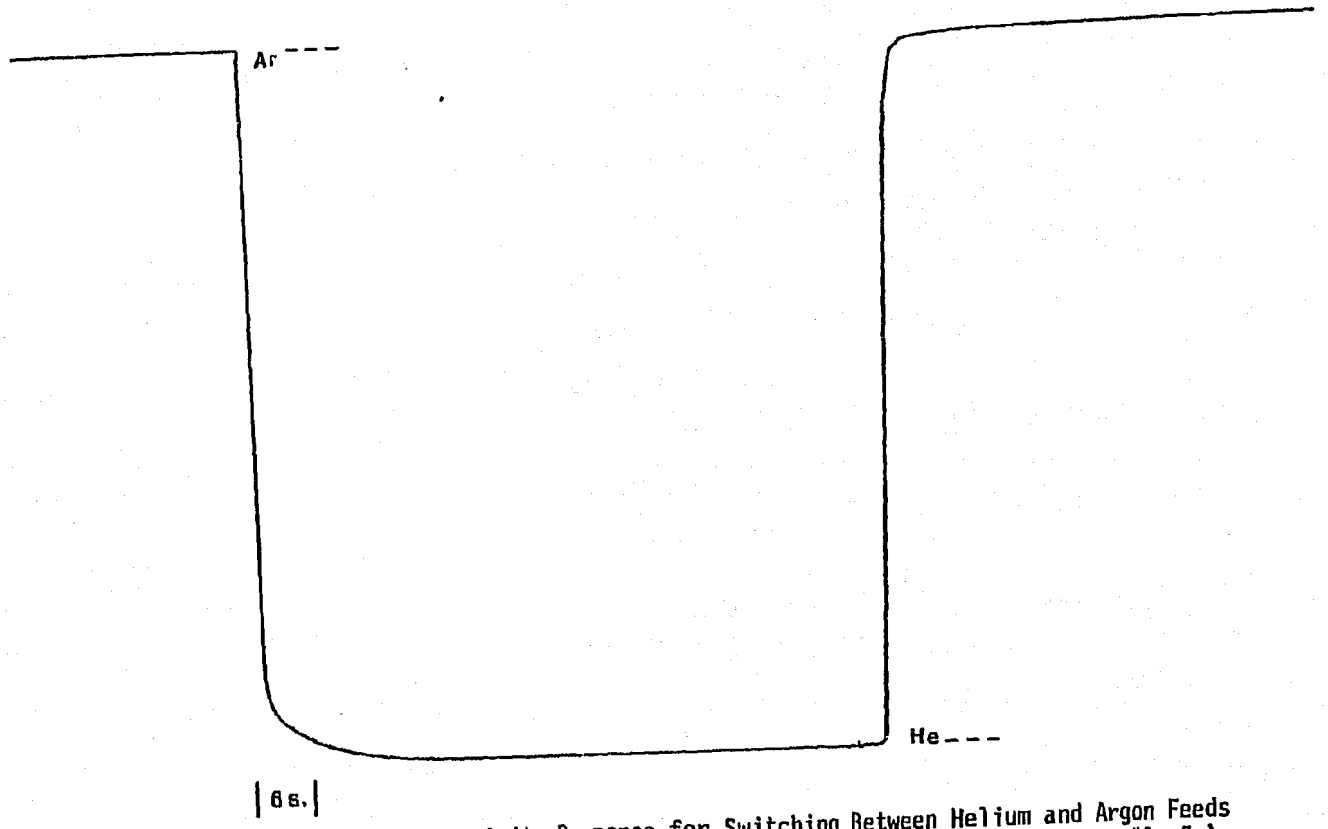

Figure F.25. The Thermal Conductivity Response for Switching Between Helium and Argon Feeds in the Cold-Flow Microreactor Model during Experiment 3-7 (Refer to Table 5.1 for the Experimental Conditions).

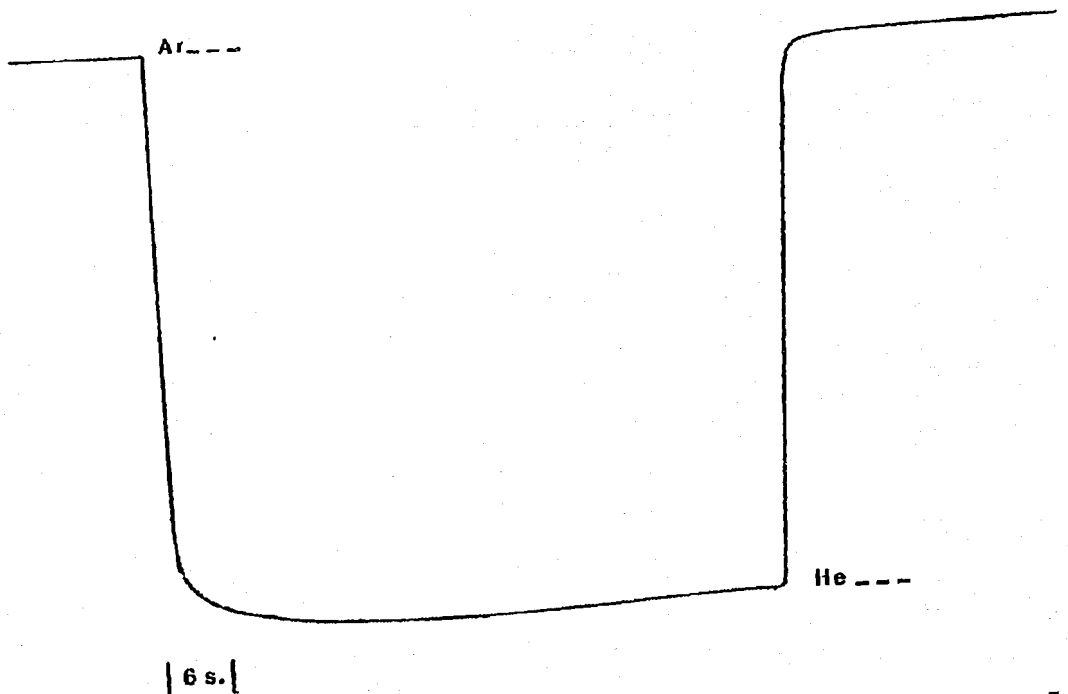

Figure F.26. The Thermal Conductivity Response for Switching Between Helium and Argon Feeds in the Cold-Flow Microreactor Model during Experiment 3-8 (Refer to Table 5.1 for the Experimental Conditions).

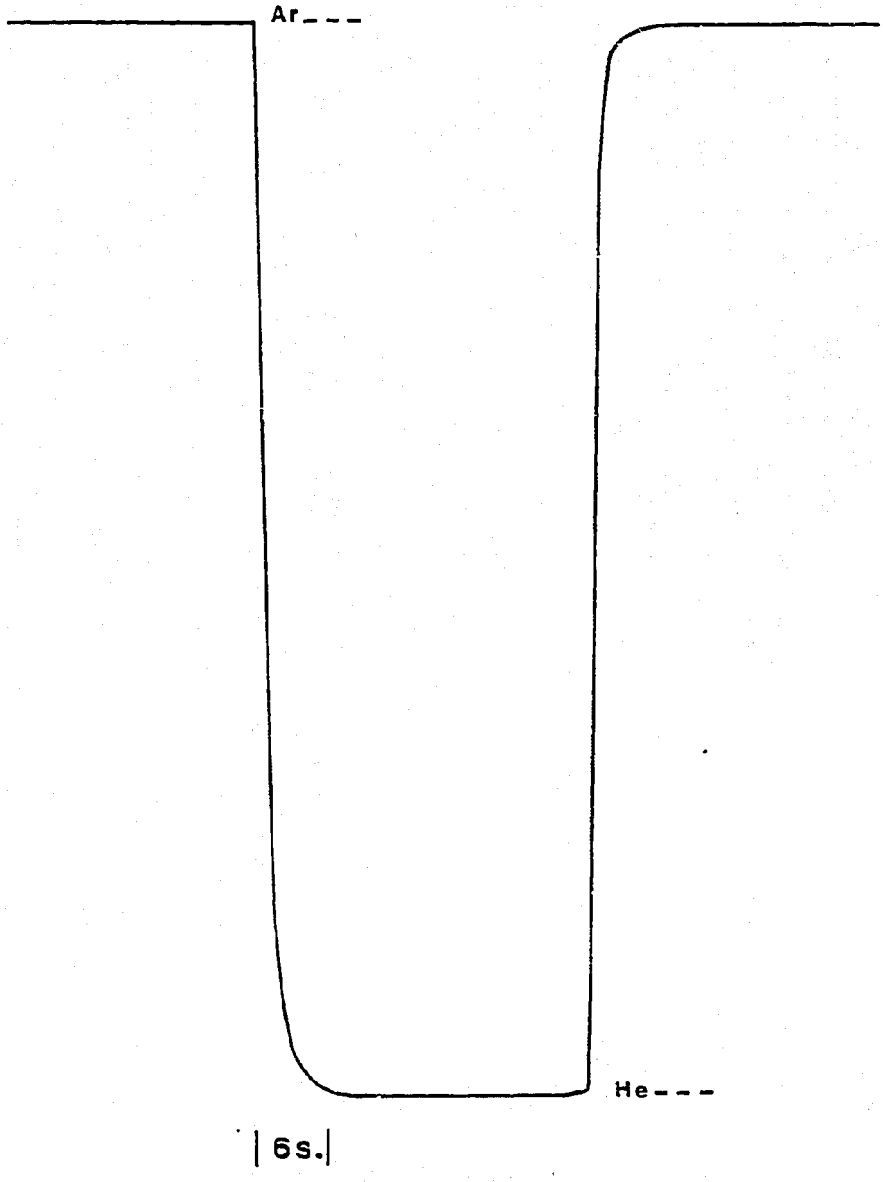

Figure F.27. The Thermal Conductivity Response for Switching Between Helium and Argon Feeds in the Cold-Flow Microreactor Model during Experiment 3-9 (Refer to Table 5.1 for the Experimental Conditions).

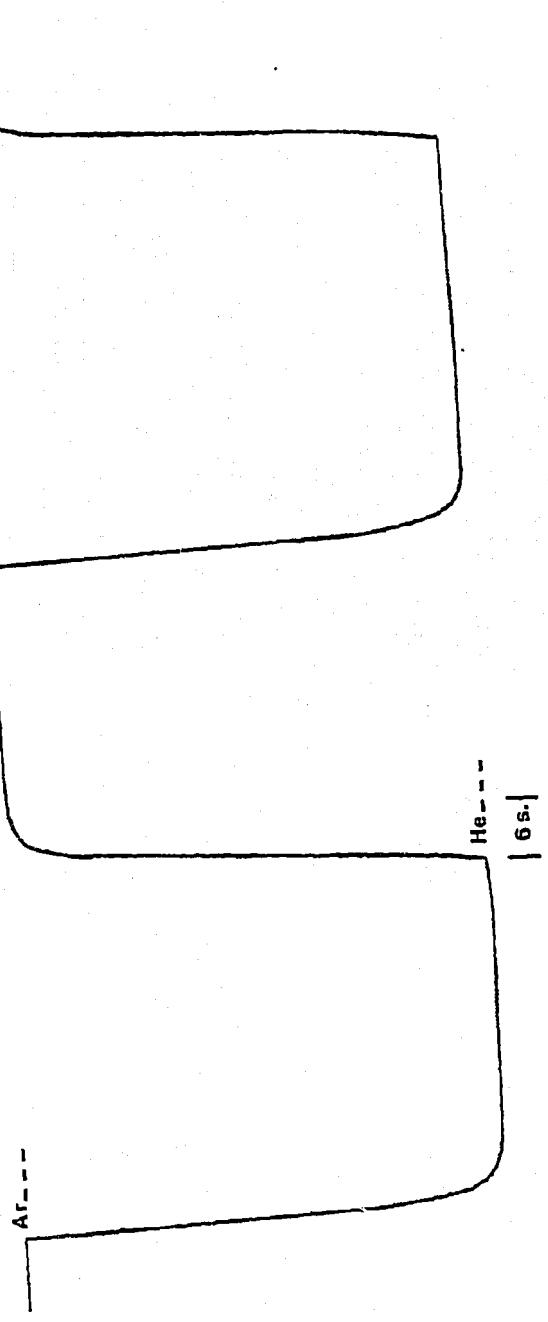

Figure F.28. The Thermal Conductivity Response for Switching Between Helium and Argon Feeds in the Cold-Flow Microreactor Model during Experiment 3-10 (Refer to Table 5.1 for the Experimental Conditions).

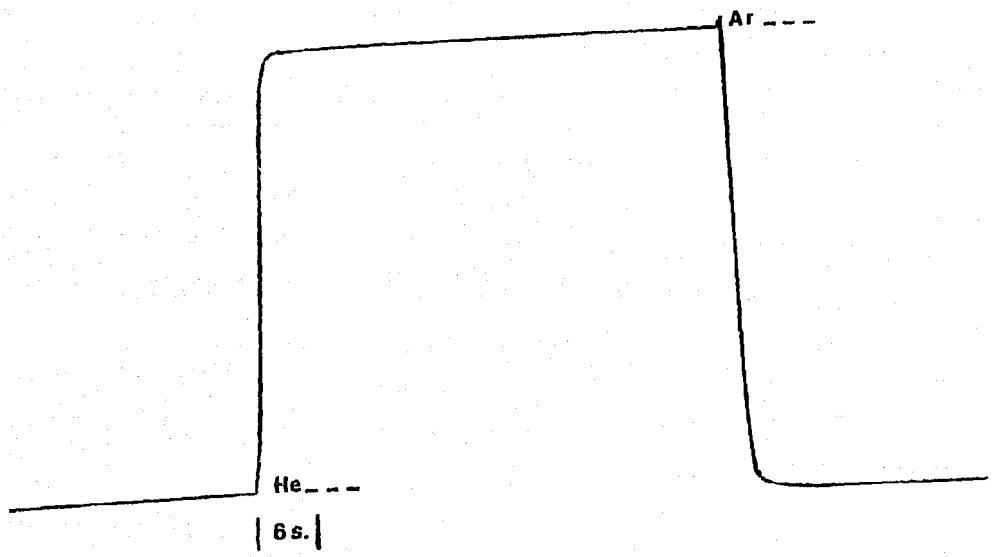

Figure F.29. The Thermal Conductivity Response for Switching Between Helium and Argon Feeds in the Cold-Flow Microreactor Model during Experiment 3-11 (Refer to Table 5.1 for the Experimental Conditions).

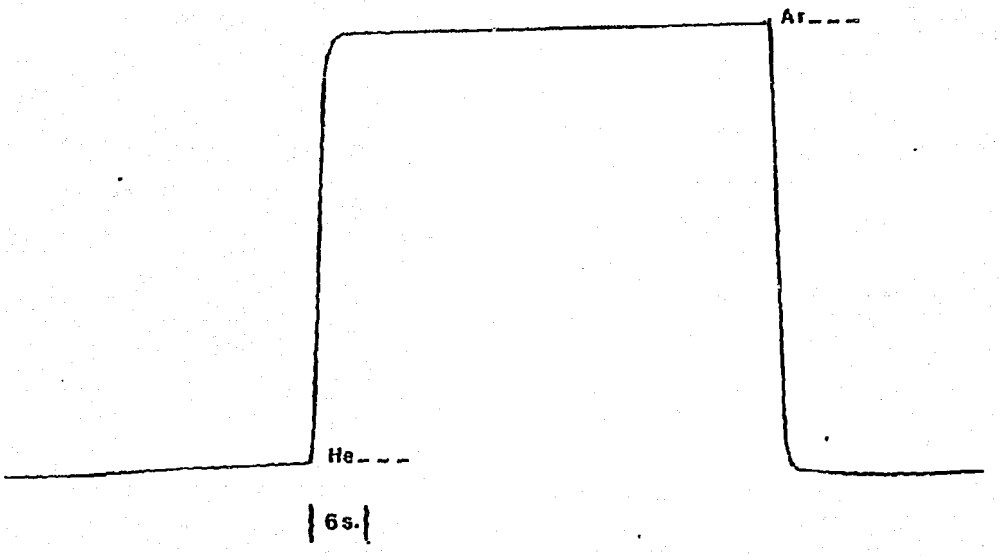

Figure F.30. The Thermal Conductivity Response for Switching Between Helium and Argon Feeds in the Cold-Flow Microreactor Model during Experiment 3-12 (Refer to Table 5.1 for the Experimental Conditions).

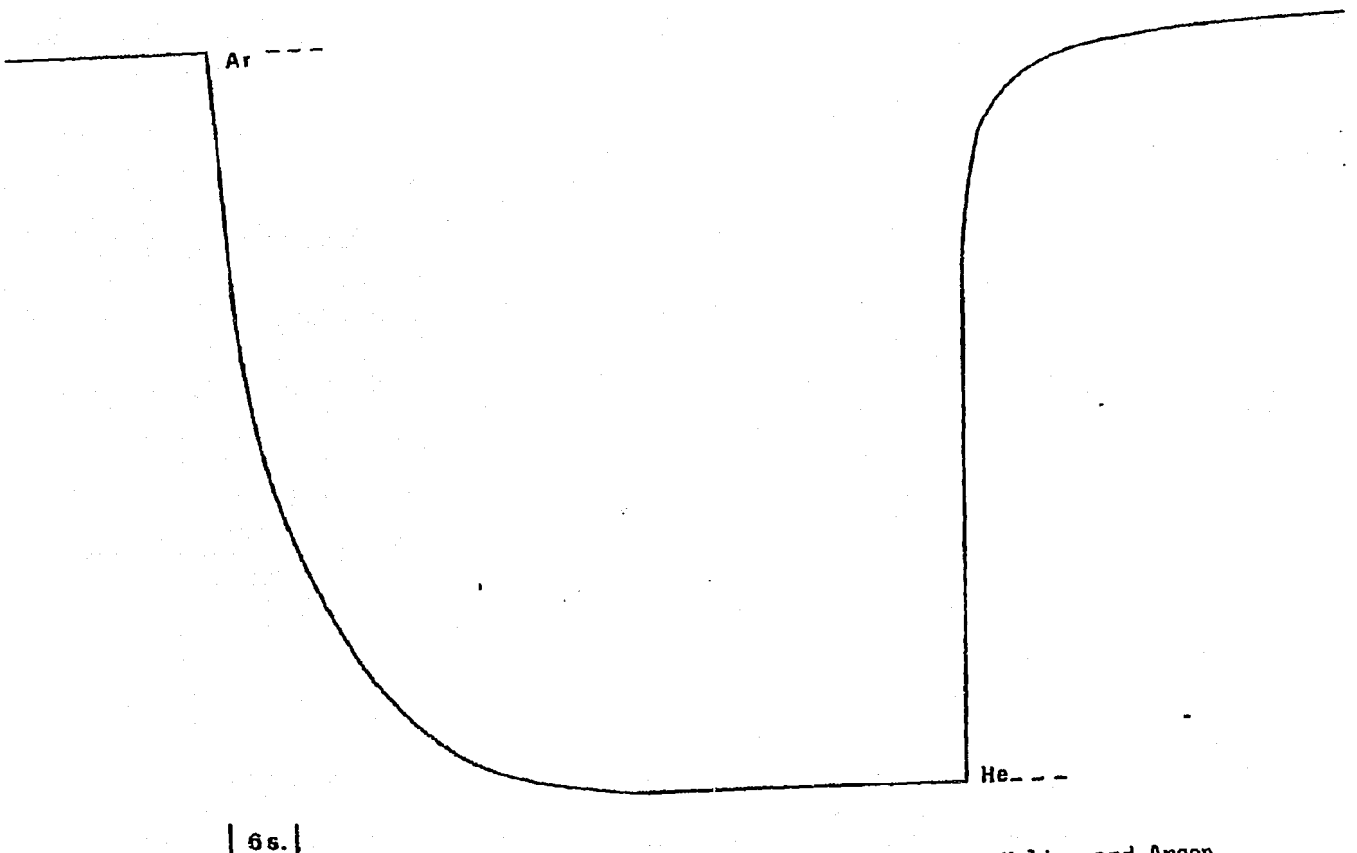

Figure F.31. The Thermal Conductivity Response for Switching Between Helium and Argon Feeds in the Cold-Flow Microreactor Model during Experiment 4-2 (Refer to Table 5.1 for the Experimental Conditions).

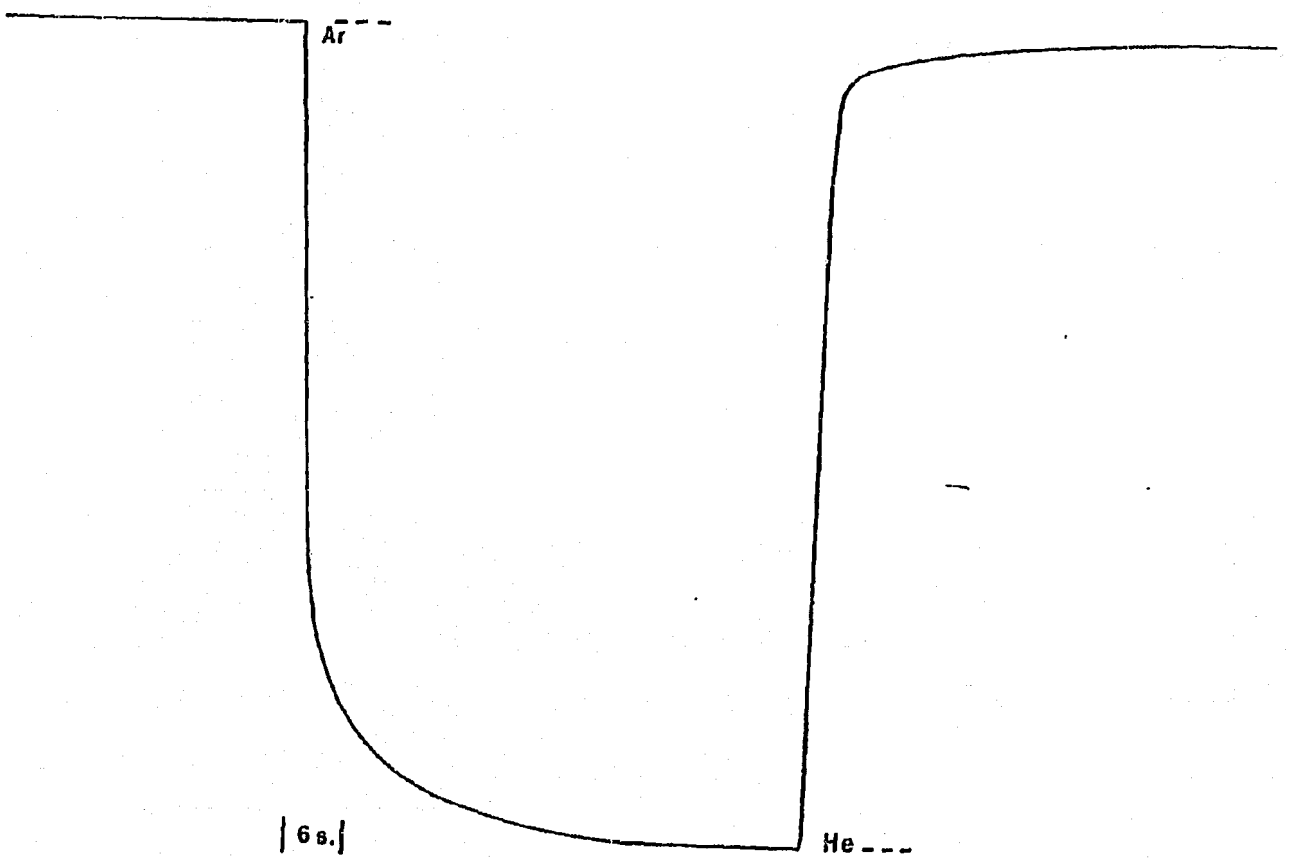

Figure F.32. The Thermal Conductivity Response for Switching Between Helium and Argon Feeds in the Cold-Flow Microreactor Model during Experiment 4-3 (Refer to Table 5.1 for the Experimental Conditions).

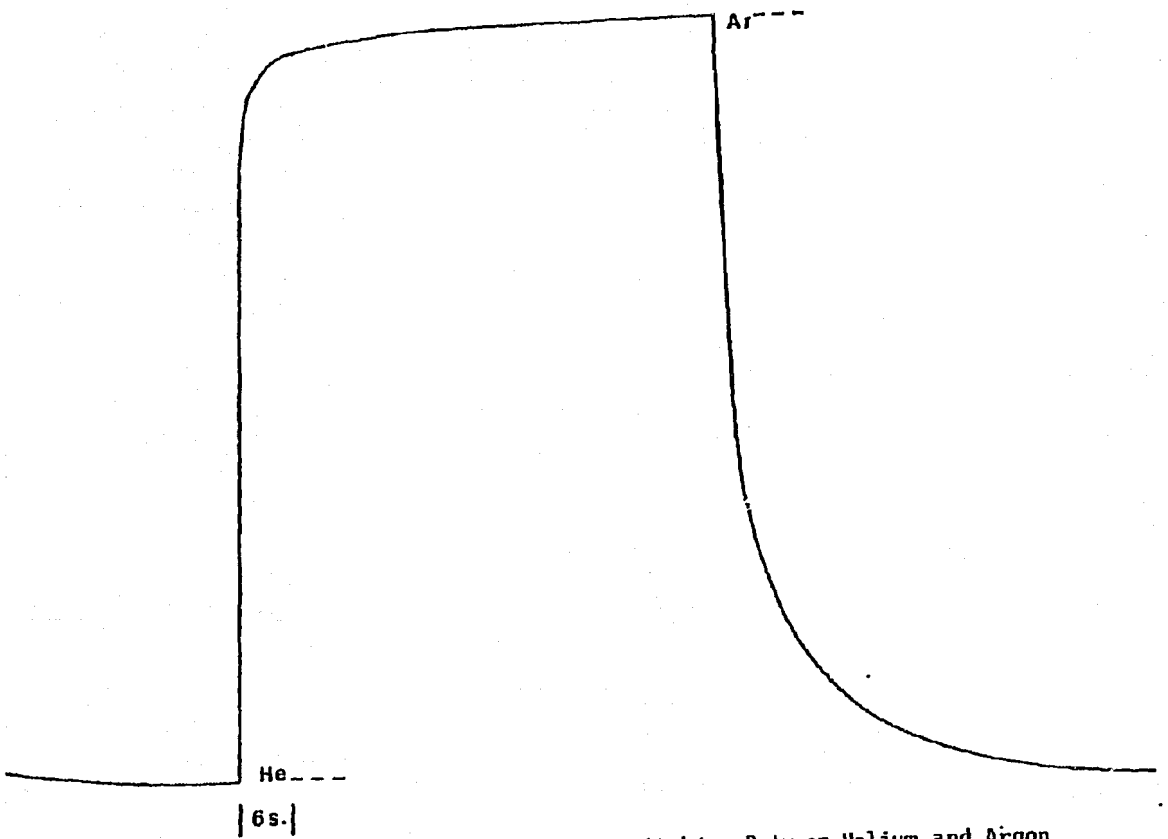

Figure F.33. The Thermal Conductivity Response for Switching Between Helium and Argon Feeds in the Cold-Flow Microreactor Model during Experiment 4-4 (Refer to Table 5.1 for the Experimental Conditions).

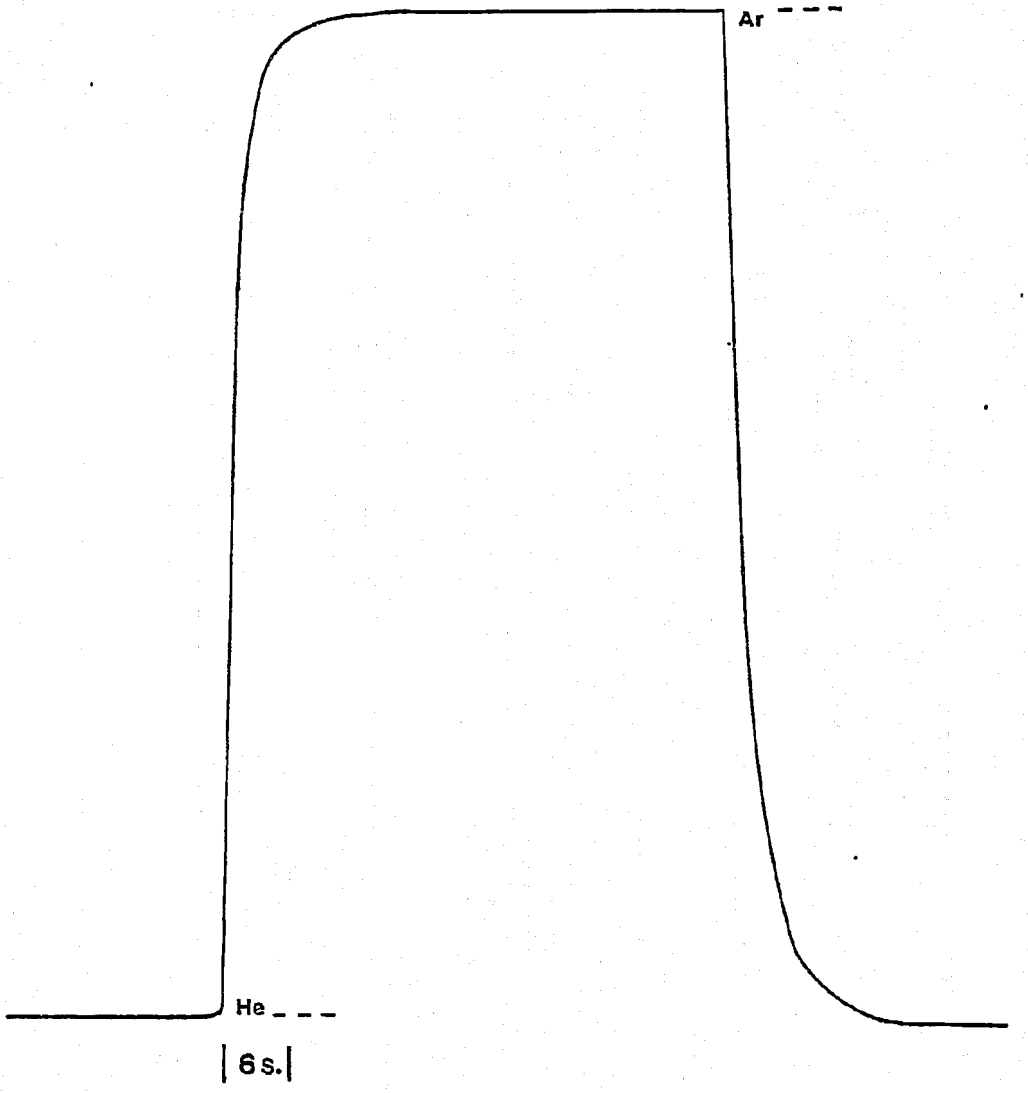

Figure F.34. The Thermal Conductivity Response for Switching Between Helium and Argon Feeds in the Cold-Flow Microreactor Model during Experiment 4-5 (Refer to Table 5.1 for the Experimental Conditions).

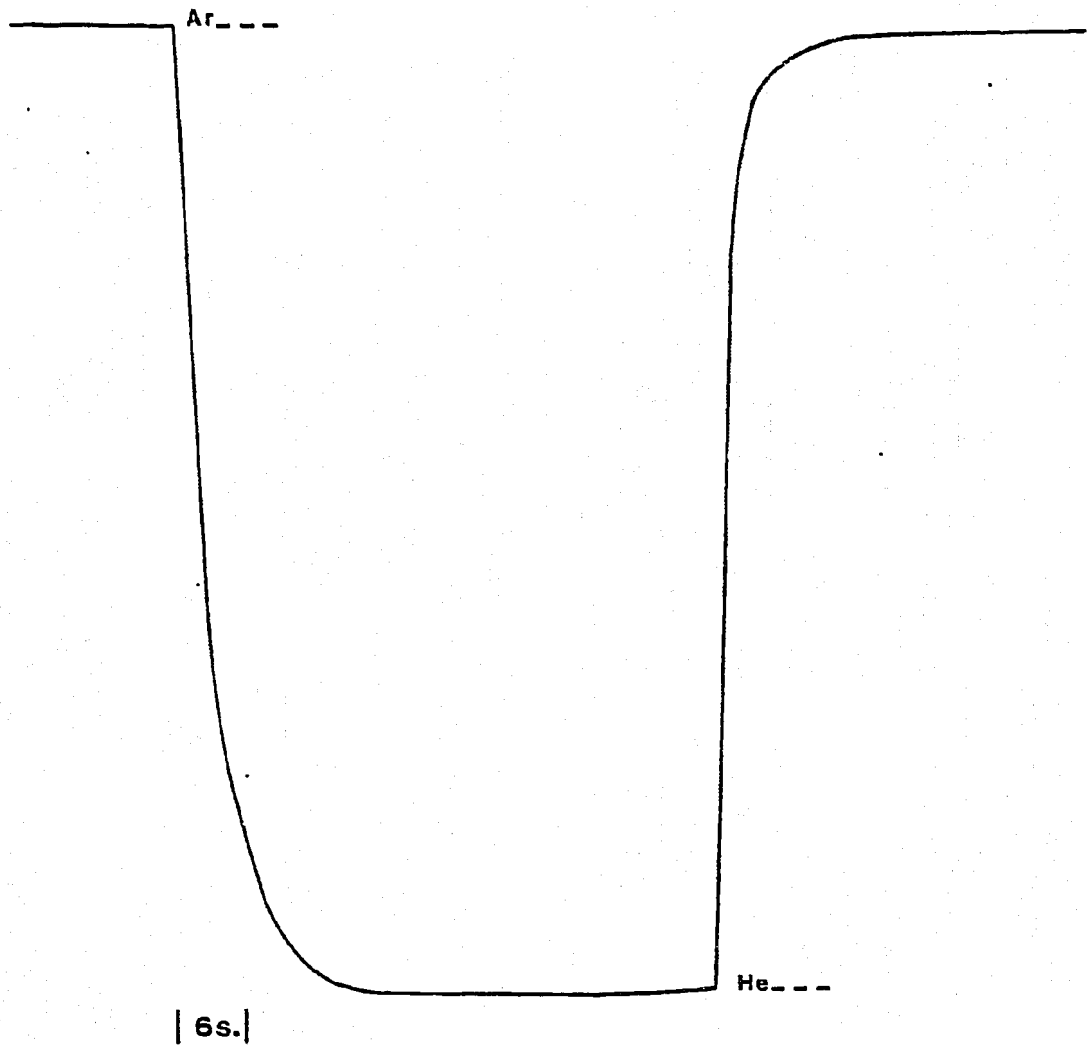

Figure F.35. The Thermal Conductivity Response for Switching Between Helium and Argon Feeds in the Cold-Flow Microreactor Model during Experiment 4-6 (Refer to Table 5.1 for the Experimental Conditions).

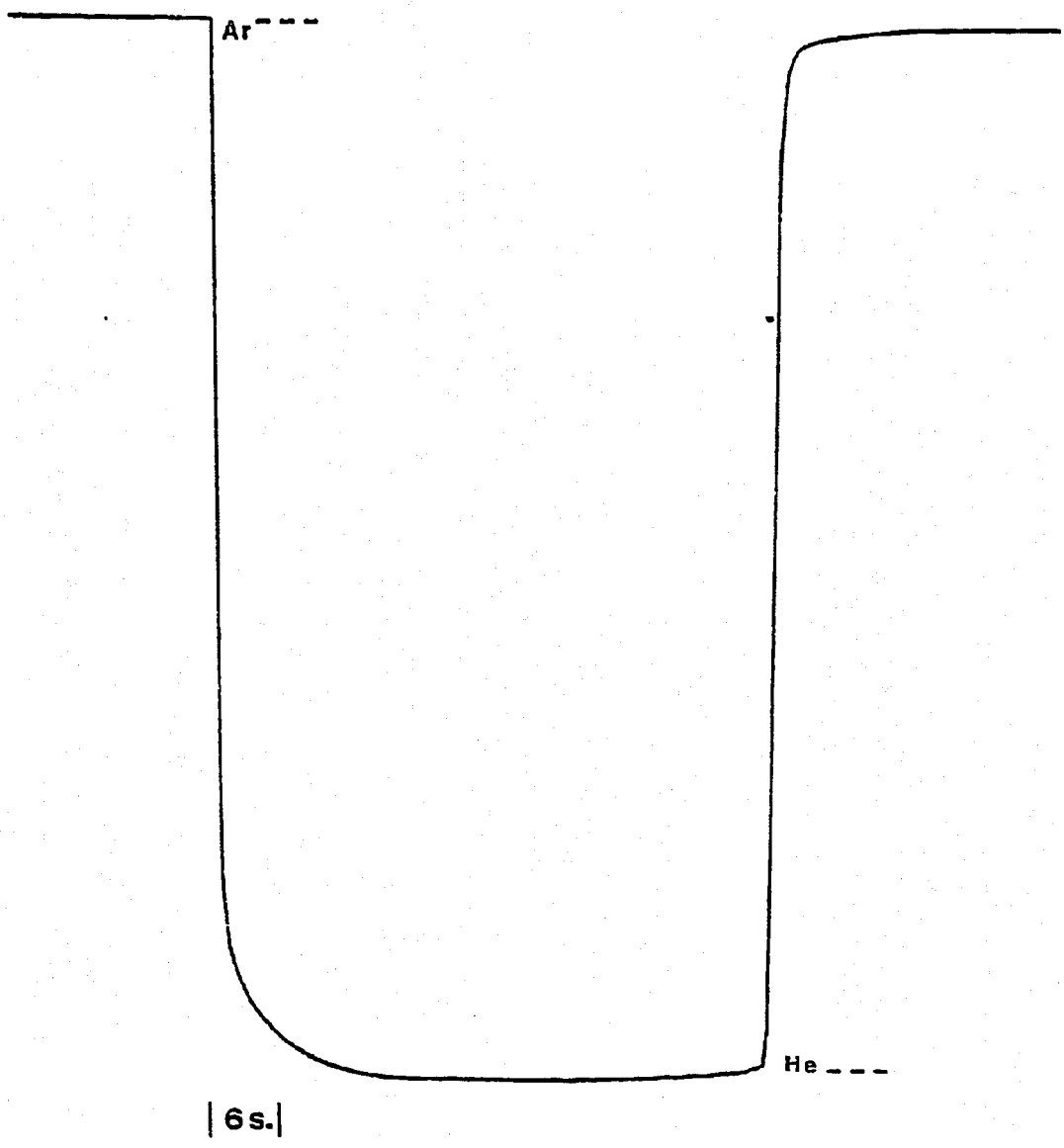

Figure F.36. The Thermal Conductivity Response for Switching Between Helium and Argon Feeds in the Cold-Flow Microreactor Model during Experiment 4-7 (Refer to Table 5.1 for the Experimental Conditions).

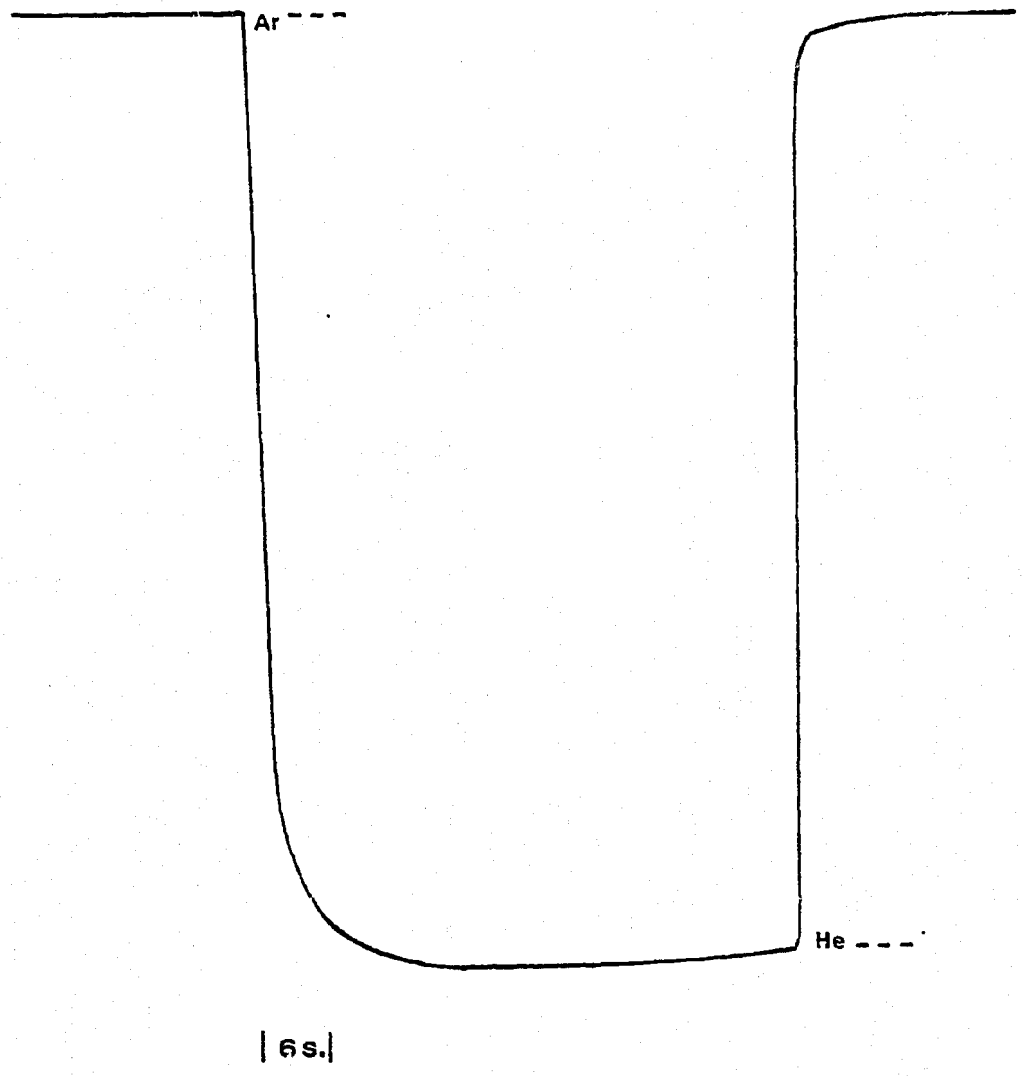

Figure F.37. The Thermal Conductivity Response for Switching Between Helium and Argon Feeds in the Cold-Flow Microreactor Model during Experiment 4-8 (Refer to Table 5.1 for the Experimental Conditions).

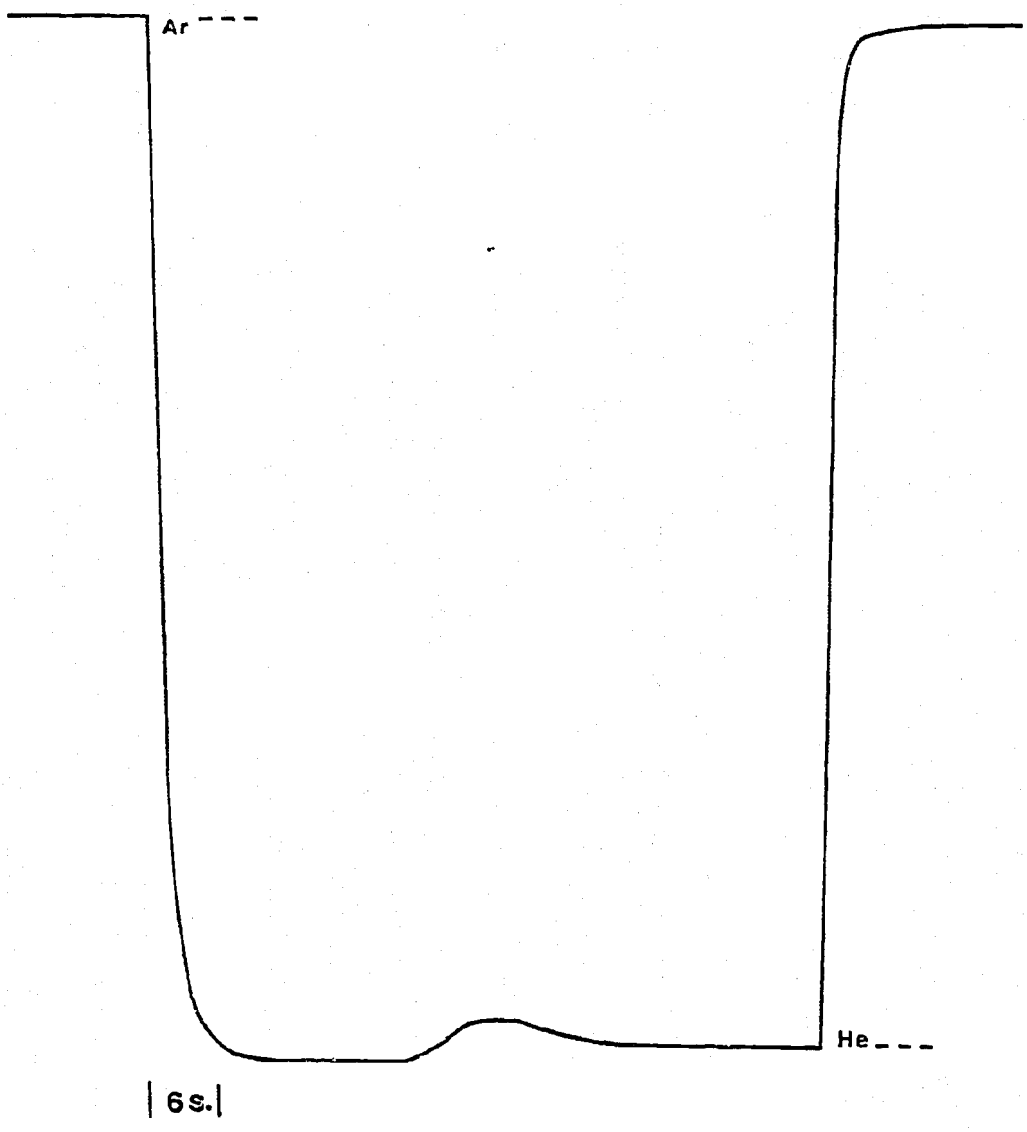

Figure F.38. The Thermal Conductivity Response for Switching Between Helium and Argon Feeds in the Cold-Flow Microreactor Model during Experiment 4-9 (Refer to Table 5.1 for the Experimental Conditions).

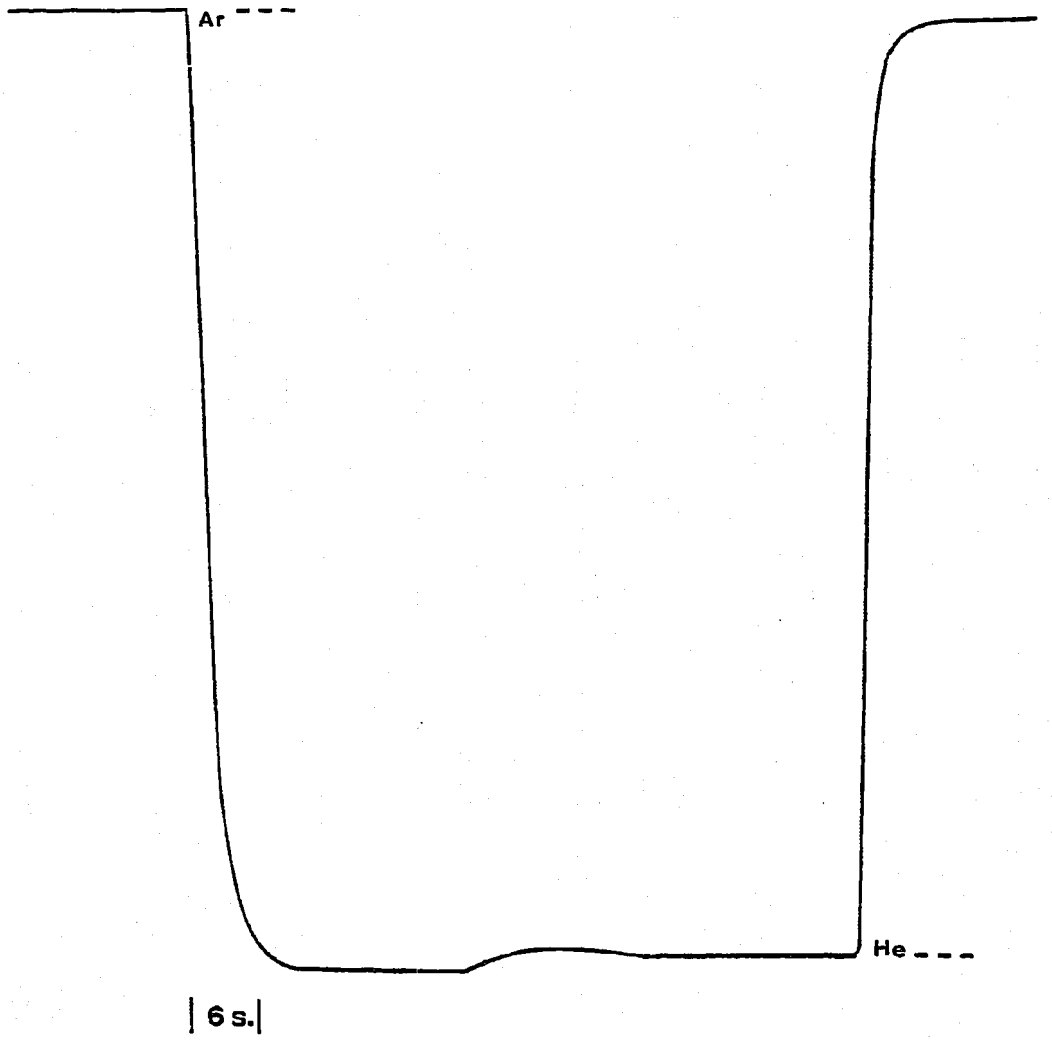

Figure F.39. The Thermal Conductivity Response for Switching Between Helium and Argon Feeds in the Cold-Flow Microreactor Model during Experiment 4-10 (Refer to Table 5.1 for the Experimental Conditions).

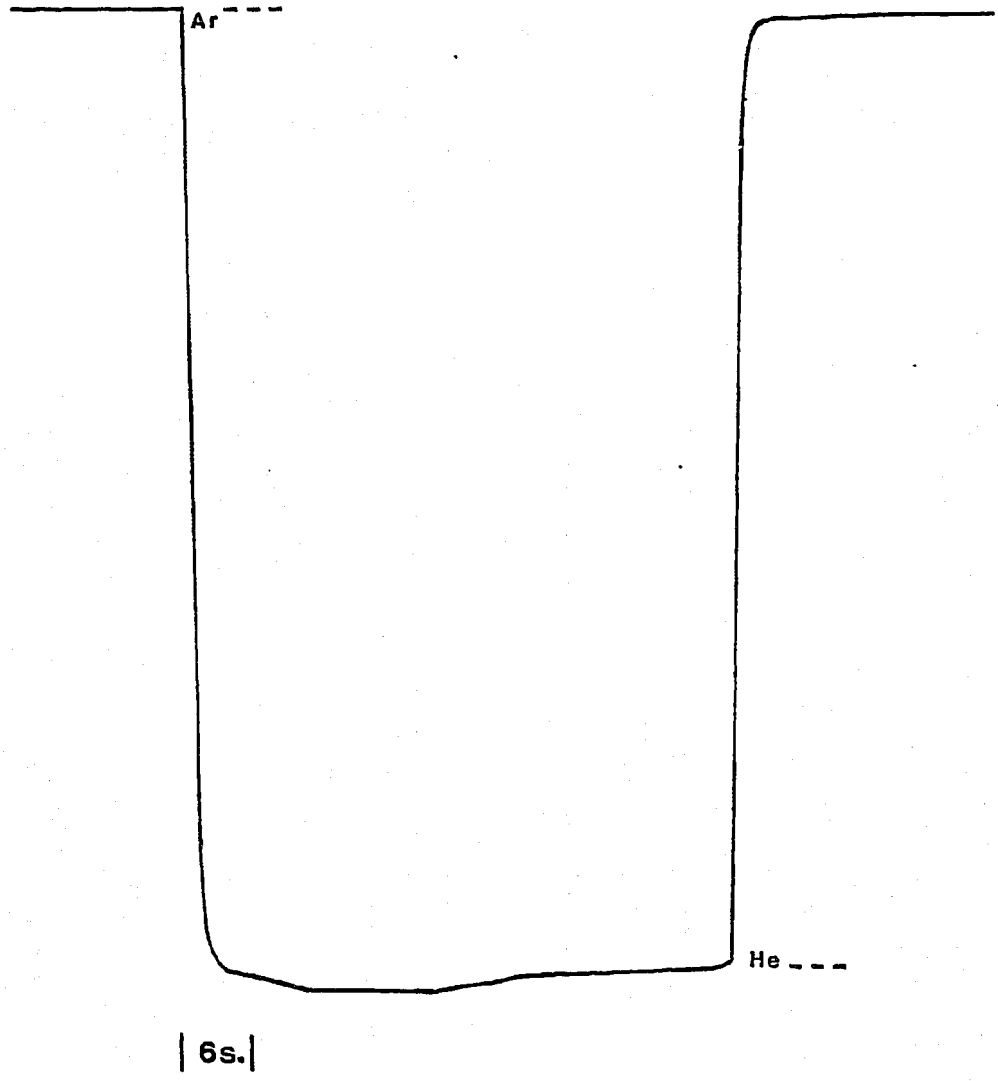

Figure F.40. The Thermal Conductivity Response for Switching Between Helium and Argon Feeds in the Cold-Flow Microreactor Model during Experiment 4-11 (Refer to Table 5.1 for the Experimental Conditions).

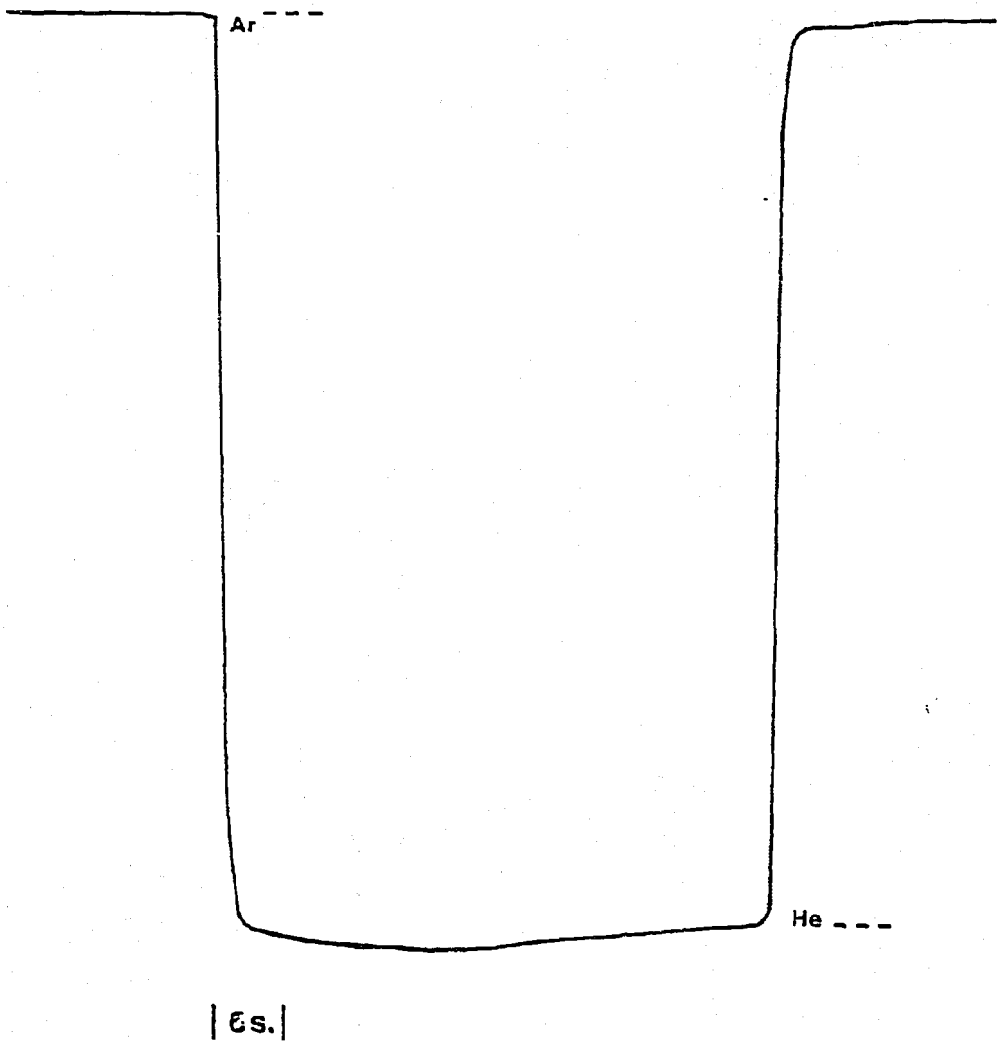

Figure F.41. The Thermal Conductivity Response for Switching Between Helium and Argon Feeds in the Cold-Flow Microreactor Model during Experiment 4-12 (Refer to Table 5.1 for the Experimental Conditions).